



Measurement report: Impact of domestic heating on dust  
deposition sources in hyper-arid Qaidam Basin, northern  
Qinghai-Xizang Plateau

Haixia Zhu<sup>abc</sup>, Lufei Zhen<sup>abc</sup>, Suping Zhao<sup>d\*</sup>, Xiyang Zhang<sup>ab\*</sup>

<sup>a</sup> Key Laboratory of Green and High-end Utilization of Salt Lake Resources, Qinghai Institute of Salt  
Lakes, Chinese Academy of Sciences, Xining, 810008, China.

<sup>b</sup> Qinghai Provincial Key Laboratory of Geology and Environment of Salt Lakes, Qinghai Institute of Salt  
Lakes, Chinese Academy of Sciences, Xining, 810008, China.

<sup>c</sup> University of the Chinese Academy of Sciences, Beijing, 100049, China

<sup>d</sup> Key Laboratory of Cryospheric Science and Frozen Soil Engineering, Northwest Institute of Eco-  
Environment and Resources, Chinese Academy of Sciences, Lanzhou, 730000, China

\* Corresponding author: E-mail address: xyzhchina@isl.ac.cn (Xiyang Zhang) and zhaosp@lzb.ac.cn  
(Suping Zhao)



23 **Highlights**

24 1. The temporal and spatial distribution of carbonaceous aerosols was analyzed using various carbon  
25 indicators.

26 2. Domestic heating significantly increased atmospheric pollutants in rural areas.

27 3. The unique energy structure in Qaidam Basin significantly influenced the glaciers of the  
28 Qinghai-Xizang Plateau and should not be overlooked.

29



30 **Abstract**

31 Given the unique energy profile of the Qaidam Basin (QDB), it is crucial to examine the impacts of  
32 domestic heating on, the Qinghai-Xizang Plateau (QXP), and global atmospheric systems. This  
33 study collected monthly dust deposition six sites in the southern QDB between 2020 and 2023. We  
34 identified the sources of dust -fall during domestic heating (HP) and non-heating periods (NHP) in  
35 urban and rural and its environmental effects. The results demonstrated that domestic heating  
36 increased the concentration of water-soluble ions in rural, trace elements in urban, and carbon  
37 emissions in both. Among various carbon indicators, organic carbon (OC) and element carbon (EC)  
38 levels rose during the HP, with Char-EC as the primary component of EC. Char-EC concentrations  
39 were higher in urban areas, while secondary organic carbon, the main contributor to OC, was more  
40 prevalent in rural. The OC/EC and char-EC/soot-EC ratios, along with PMF results, indicated that  
41 coal and biomass burning were the main contributors to dust deposition in rural, strongly influenced  
42 by domestic heating, whereas urban dust predominantly originated from vehicle and industrial  
43 emissions. Coal consumption in QDB was greater during the HP than that of other dust sources in  
44 the QXP. This increased consumption leads to higher emissions of atmospheric pollutions, which  
45 may accelerate glacier melting in the region. Consequently, integrating QDB carbon aerosols into  
46 future environmental policies and climate models for the QXP is essential. This study provides a  
47 reference for investigating carbonaceous aerosols in climatically similar hyper-arid basins with  
48 intensive human activity and salt lake regions.

49 **Keywords**: Qinghai-Xizang Plateau; Qaidam Basin; Biomass burning; carbonous elements;  
50 atmospheric deposition.

51



52    **Short summary**

53    This study collected dust samples from six sites in the Qaidam Basin, over three years to investigate  
54    the impact of domestic heating on atmospheric dust in hyper-arid region. Our results indicate that  
55    rural dust is significantly influenced by heating, particularly from coal and biomass burning which  
56    accounts for over 70% of total sources. The unique energy structure here has resulted in distinct  
57    environmental effects from the emitted carbonaceous aerosols and useful for similar dry areas.



## 58 1. Introduction

59 Atmospheric dust, a critical component of particulate matter (PM), serves as both an air quality  
60 indicator and environmental stressor, influencing hydrological cycles and soil ecosystems (Feng et  
61 al., 2019). Recent advancements in understanding PM characteristics—particularly chemical  
62 composition (e.g. water-soluble ions, organic carbon, and elemental carbon) and source  
63 apportionment—have been achieved through principal component analysis (PCA), chemical mass  
64 balance (CMB), and positive matrix factorization (PMF) models (Lai et al., 2016; Yao et al., 2016a;  
65 Zhang et al., 2015b). PMF analysis of atmospheric dust in urban such as Lanzhou, Taiyuan, and  
66 Jinan have identified diverse sources, including coal combustion, industrial emissions, construction  
67 dust, windblown dust, vehicle emissions, and resuspended road dust. Seasonal variations indicate  
68 that coal combustion during the domestic heating period and regional meteorological conditions  
69 significantly influence dust deposition (Hu and Liu, 2022; Chen et al., 2024; Yang et al., 2024;  
70 Zhang et al., 2022). These findings underscore the urgency of region-specific pollution control  
71 strategies.

72 The Qinghai-Xizang Plateau (QXP) is a key regulator of Northern Hemisphere climate  
73 variability and plays a vital role in global ecological and climatic stability, often referred to as the  
74 “Asian Water Tower” (Liu et al., 2019; Liu et al., 2020b). However, rapid glacier retreat on the  
75 plateau poses risks to the Asian hydrological cycle and the monsoon system, with potential adverse  
76 impacts if unchecked (Luo et al., 2020). Beyond climate warming and increased humidity, black  
77 carbon (BC) significantly accelerates glacial melt by inducing atmospheric warming and enhancing  
78 radiative absorption at the glacier surface (Bond and And Bergstrom, 2006; Chen et al., 2015).  
79 Notably, biomass burning in South and Central Asia during winter serves as a major source of BC,  
80 further exacerbating glacier decline on the plateau (Zhang et al., 2015c; Zheng et al., 2017; Xu et  
81 al., 2018b). However, local sources within the QTP, particularly the Qaidam Basin (QDB) in the  
82 northeastern region, should not be underestimated, as QDB is a key dust source for the plateau (Wei  
83 et al., 2017; Zheng et al., 2021).

84 The QDB, known as the “Treasure Bowl” of the QXP, is rich in minerals, coal, oil, and gas,  
85 positioning it a key economic hub in northwest China. It has a high population density, and intense  
86 human activity, yet is highly sensitive to climate change. Extensive resource extraction has rendered



87 its ecosystem fragile (Li and Sha, 2022), exacerbating atmospheric pollution. Unlike South Asia,  
88 Central Asia, and Xizang—where biomass fuels dominate—QDB relies primarily on a mixture of  
89 coal, yak dung, and firewood for winter domestic heating, reflecting a unique energy structure (Liu  
90 et al., 2008; Xiao et al., 2015; Behera et al., 2015; Kerimray et al., 2018; Jiang et al., 2020; Shen et  
91 al., 2021). The combustion of coal releases significant pollutants, light-absorbing organic  
92 compounds like BC and brown carbon, and hazardous gases such as carbon dioxide (CO<sub>2</sub>),  
93 nitrogen oxides (NO<sub>x</sub>) and carbon monoxide (CO). These emissions impact human health and  
94 exacerbate climate warming, thereby influencing regional and global climate systems (Munawer,  
95 2018; Ye et al., 2020; Zhou et al., 2025). Consequently, we posit that seasonal carbon emissions in  
96 QDB, particularly during winter domestic heating, could exert a unique influence on the climate  
97 and ecological stability of the QXP.

98 Additionally, the QDB as a representative arid region with intensive human activity, exhibits  
99 climatic and environmental conditions comparable to the Tarim and Junggar Basins in Xinjiang, the  
100 Great Basin in the United States, and other hyper-arid areas. These regions are characterized by low  
101 precipitation, rich mineral resources subject to significant anthropogenic impact, and abundant salt  
102 lakes. Similarly, salt lakes such as the Uyuni in Bolivia, Atacama in Chile, and Ombre-Muerto in  
103 Argentina are located on high plateaus averaging 3,000 m in elevation, with surrounding climates  
104 and environments comparable to those of the QDB. Research in the Tarim and Junggar Basins has  
105 predominantly focused on dust events, their sources, and associated gas emissions (Gao and  
106 Washington, 2010; Liu et al., 2016b; Filonchyk et al., 2018; Yu et al., 2019; Zhou et al., 2023). In  
107 the Great Basin, studies largely address ozone and dust sources (Hahnenberger and Nicoll, 2012;  
108 Vancuren and Gustin, 2015; Miller et al., 2015). Research on salt lake atmospheres has  
109 predominantly focused on high-salinity dust emissions resulting from lakebed desiccation due to  
110 resource extraction (Löw et al., 2013; Gholampour et al., 2015; Moravek et al., 2019; Christie et al.,  
111 2025), with limited research on atmospheric carbon components, their sources, and environmental  
112 impacts. Therefore, this research aims to investigate atmospheric carbonaceous aerosols in arid  
113 basins with intensive human activity and climates comparable to the QDB, as well as in salt lakes  
114 environments.

115 This study, conducted from January 2020 to March 2023, involved monthly dust deposition  
116 sampling at six urban and rural monitoring sites located in the southern QDB. Samples were



117 categorized into two seasonal periods: the domestic heating (HP) and the non-domestic heating  
118 (NHP) periods. The HYSPLIT model, and PMF receptor modeling using analyses of dust flux,  
119 soluble ions, trace elements, and carbonaceous components, alongside OC/EC and char/soot  
120 ratios—the primary sources of dust deposition were identified, with particular emphasis on  
121 contributions from domestic heating. The study further evaluated the environmental impacts on the  
122 QXP, considering its distinctive energy structure. Furthermore, These findings offer a scientific basis  
123 and reference for examining atmospheric carbonaceous aerosols in arid basins with similar climates  
124 and human activities to the QDB, as well as in salt lake regions.

125

## 126 **2. Materials and methods**

### 127 **2.1 Sampling**

128 The QDB, situated in the northeastern of the QXP, is bordered by the Altyn-Tagh, Kunlun, and  
129 Qilian mountains, making it one of China's largest intermontane basins (Zhang, 1987). With an  
130 average elevation of 3,000 m, the basin features an extremely arid climate characterized by less than  
131 20 mm of annual precipitation in the northwestern region, while evaporation rates exceed 2,000 mm.  
132 The QDB is rich in salt lakes, non-ferrous metals, and hydrocarbon resources, with significant coal  
133 deposits. It leads China in reserves of halite, potash, magnesium, lithium, strontium, asbestos,  
134 earning it the nickname “Treasure Basin”. As a major salt lake resource area, it hosts 33 lakes—  
135 including Qarhan, Daqingkan, and Caka Salt Lake—and faces notable conflicts between resource  
136 extraction and ecological preservation. Agriculturally, it cultivates crops like goji berries, quinoa,  
137 and forage grass, and hosts China’s largest resource-rich circular economy pilot zone. The  
138 permanent population of basin is approximately 400,000, primarily using coal, yak dung, and  
139 firewood for domestic heating (Jiang et al., 2020). Additionally, annual tourism peaks from May to  
140 September, attracting around 17 million visitors, which likely amplifies atmospheric pollutant  
141 emissions.

142 From January 2020 to March 2023, monthly dust deposition samples were collected from six  
143 monitoring stations in the southern QDB. The stations included Xiao Zaohuo (XZH), Golmud  
144 (GEM), Da Gele (LTC), Nuo Muhong (NMH), Balong (BLX), and Dulan station (DLX). Dry  
145 deposition collection employed the glass ball method using [Marble dust collector](#) (MDCO) designed



146 dust collection cylinders (Sow et al., 2006). The stainless steel collection device (50×30×30 cm)  
147 contained a plastic sieve container of identical dimensions, with the sieve base positioned 10 cm  
148 above the opening and perforated with 0.5 cm diameter holes (Figure S1). To minimize dust  
149 resuspension during high wind events (Qian and Dong, 2004), two layers of 16 mm glass balls were  
150 placed within the sieve container. A high-density polyethylene bag was attached to the base for  
151 sample collection.

152 To ensure only dry dust was collected, collection devices were covered during rain or snowfall.  
153 A total of 37, 39, 23, 30, 16, and 29 samples were obtained from XZH, GEM, LTC, NMH, BLX,  
154 and DLX stations, respectively. Laboratory protocols incorporated biannual analyses with negative  
155 controls and appropriate control samples. As continuous dust monitoring commenced in 2020, site  
156 blanks were evaluated during initial sampling. Stations were classified as Urban (GEM, NMH, DLX)  
157 and Rural (XZH, LTC, BLX) based on location characteristics. Consistent with the cold-arid climate  
158 in QDB, the HP was defined as October-April, while the NHP spanned May-September.

159 Materials such as plant remnants, microfauna, and bird droppings were removed from the  
160 sample bags with tweezers. The samples were then measured on a balance (0.0001 g) to determine  
161 the dust deposition flux (Eq. 1) (Yu et al., 2016):

$$162 \quad M = \frac{m \times 30}{S \times K}, \quad (1)$$

163 where M is dust deposition [ $\text{g}/(\text{m}^2 \cdot 30\text{d})$ ]; m is the sample mass (g); S is the area of the dust collection  
164 device ( $\text{m}^2$ ); and K is the actual number of sampling days per month (d).



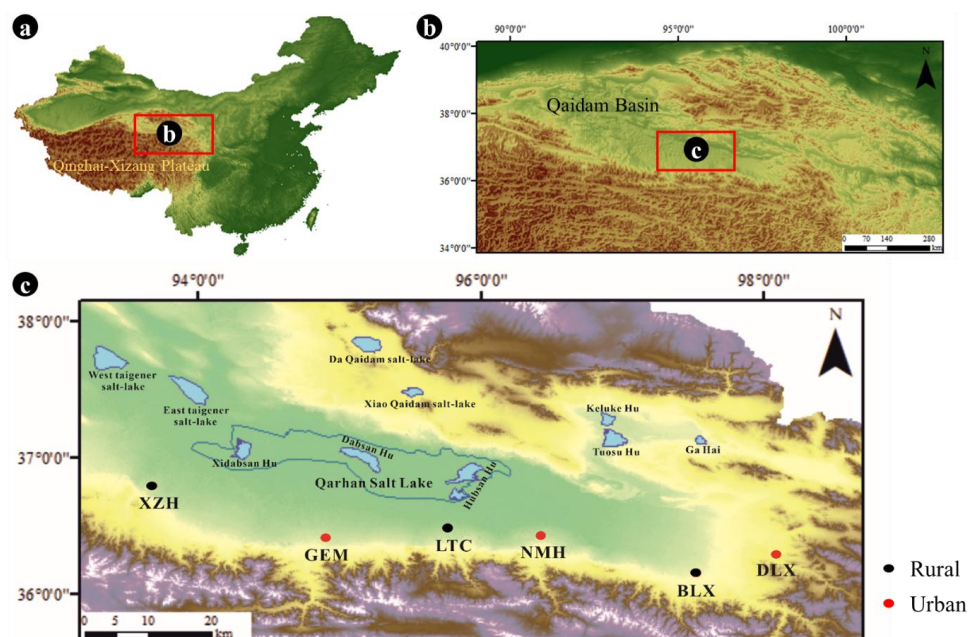


**Figure 1.** Spatial distribution of monitoring stations in the southern Qaidam Basin. Urban stations (red) and rural stations (black) are labeled as follows: XZH (Xiao Zaohuo), GEM (Golmud), LTC (Da Gele), NMH (Nuo Muhong), BLX (Balong), DLX (Dulan).

## 2.2 Water-soluble inorganic ions

A 100 mg sample was weighed and transferred into a 250 mL bottle. The mixture underwent ultrasonic extraction for 20 minutes to ensure complete solubilization. The resulting supernatant was then filtered through a 0.45  $\mu\text{m}$  filter for analysis. Based on preliminary experimental results, the concentrations of major ions ( $\text{K}^+$ ,  $\text{Na}^+$ ,  $\text{Mg}^{2+}$ , and  $\text{Ca}^{2+}$ ) were measured using Inductively Coupled Plasma Optical Emission Spectrometer (ICP-OES, NexIon 2000). Anions ( $\text{Cl}^-$ ,  $\text{SO}_4^{2-}$ , and  $\text{NO}_3^-$ ) were quantified using ion chromatography (IC). To ensure measurement accuracy, samples were organized in sets of twenty, with one randomly selected sample from each group serving as a replicate, achieving an error margin of less than 10%. The detection limits for the various components were as follows:  $\text{K}^+$  (0.0560 mg/L),  $\text{Na}^+$  (0.0100 mg/L),  $\text{Ca}^{2+}$  (0.0037 mg/L),  $\text{Mg}^{2+}$  (0.0390 mg/L),  $\text{SO}_4^{2-}$  (0.0090 mg/L),  $\text{NO}_3^-$  (0.0125 mg/L),  $\text{Cl}^-$  (0.0100 mg/L). All standard solutions employed in the analysis were sourced from the National Standard Material Center.



182

### 183 **2.3 Trace element analysis**

184 According to the Chinese State Standard “Ambient Air and Waste Gas from Stationary Sources  
185 Emission - Determination of Metal Elements in Ambient Particles” (HJ 777-2015), the  
186 concentrations of elements such as iron (Fe), aluminum (Al), silicon (Si), titanium (Ti), copper (Cu),  
187 cadmium (Cd), chromium (Cr), manganese (Mn), nickel (Ni), zinc (Zn), lead (Pb), and vanadium  
188 (V) were quantified using Inductively Coupled Plasma Mass Spectrometry (ICP-MS) and ICP-OES.  
189 A dust sample weighing 0.100 g was placed in a Teflon cup, to which 20.0 mL of a nitric acid-  
190 hydrochloric acid digestion solution was added. The sample was heated to reflux at  $100 \pm 5^\circ\text{C}$  for 2  
191 h under a watch glass, then cooled. Following this, the inner walls of the cup were rinsed with water,  
192 and approximately 10 mL of water was added, allowing the mixture to stand for 30 minutes for  
193 extraction. The extract was then filtered into a 100 mL volumetric flask and diluted to volume with  
194 distilled water for analysis. In cases where organic matter content was high, an appropriate amount  
195 of hydrogen peroxide was introduced during digestion to decompose the organic materials. Prior to  
196 sample analysis, the system was flushed with a rinse solution until the blank intensity value reached  
197 a minimum, and samples were analyzed only after the signal stabilized. If the concentration of any  
198 element exceeded the calibration range, the sample was diluted and reanalyzed.

199

### 200 **2.4 Carbon analysis**

201 This study utilized a combination of wet chemical treatment and thermal/optical reflection  
202 (TOR) to analyze trace elements in dust deposition (Han et al., 2007b; Han et al., 2007a; Han et al.,  
203 2016). Dust samples were treated with hydrochloric and hydrofluoric acids to remove inorganic  
204 materials. The residual solution was then filtered through a pre-combusted quartz fiber filter  
205 (Whatman,  $450^\circ\text{C}$  for 4 h, diameter 47 mm). The filtered samples were air-dried and analyzed for  
206 carbon content using a DRI 2001 thermal/optical carbon analyzer (Atmoslytic Inc., Calabasas, CA)  
207 at the Institute of Earth Environment, Chinese Academy of Sciences, adhering to the Interagency  
208 Monitoring of Protected Visual Environments (IMPROVE) protocol.

209 A  $0.544\text{ cm}^2$  disc was extracted from the filter and placed in a quartz boat for analysis. During  
210 the carbon analysis, the samples were initially heated in a 100% helium atmosphere, resulting in the



211 production of four organic carbon (OC) fractions (OC1, OC2, OC3, and OC4) at four different  
212 temperature levels (140, 280, 480, and 580 °C). The atmosphere was subsequently changed to 2%  
213 O<sub>2</sub>/98% He, generating three elemental carbon (EC) fractions (EC1, EC2, and EC3) at three  
214 temperatures (580, 740, and 840 °C). Volatile carbon underwent carbonization in an anaerobic  
215 environment, indicated by a decrease in laser reflectance, and is referred to as "pyrolyzed organic  
216 carbon" (OPC). In the oxidative atmosphere, OPC was emitted along with the original EC from the  
217 filter. The amount of OPC is defined as the carbon evolved until the laser reflectance returned to its  
218 baseline value (Han et al., 2007b). According to the IMPROVE protocol, EC is calculated as the  
219 total of the three EC subfractions minus OPC (i.e., EC = EC1+EC2+EC3-OPC). The method enables  
220 differentiation between soot and ash, as determined by the gradual oxidation of these black carbon  
221 subtypes in standard reference materials during the EC1 and EC2 + EC3 steps, where soot is defined  
222 as EC1-OPC and ash as EC2+EC3 (Han et al., 2007a; Han et al., 2016).

223 Please note that in this manuscript, we interchangeably use the terms "EC" and "BC." While  
224 these terms do not strictly refer to the same component, they serve as an adequate approximation  
225 within the scope of this study (Seinfeld et al., 1998; Bond et al., 2004). We use "EC" when discussing  
226 emissions and modeling components, reserving "BC" for climate-related discussions.

227

## 228 **2.5 Statistical analysis**

### 229 (1) Estimation of Secondary Organic Carbon

230 OC consists of primary organic carbon (POC) and secondary organic carbon (SOC). An OC/EC  
231 ratio exceeding 2.0 indicates the possible presence of secondary organic aerosol (SOA) (Castro et  
232 al., 1999). Due to the intricate physical and chemical processes involved, SOC in urban atmospheres  
233 cannot be directly measured. Therefore, an indirect estimation method, known as the EC tracer  
234 method, has been developed (Turpin and Huntzicker, 1991). If the concentrations of OC and EC are  
235 available and primary OC from non-combustion sources (OC<sub>non-comb</sub>) can be disregarded, EC can be  
236 utilized as a tracer for POC from combustion sources, facilitating the estimation of SOC (Turpin  
237 and Huntzicker, 1995):

$$238 \quad \text{POC} = \text{EC} \times (\text{OC}/\text{EC})_{\text{pri}}, \quad (2)$$

$$239 \quad \text{SOC} = \text{OC}_{\text{total}} - \text{POC}, \quad (3)$$



where  $OC_{\text{total}}$  represents total organic carbon. Traditional methods for determining  $(OC/EC)_{\text{pri}}$  involve regressing OC and EC within a fixed percentile range of the lowest  $(OC/EC)$  ratio data (typically 5-20%) or relying on sampling days characterized by low photochemical activity and local emissions (Castro et al., 1999; Lim and Turpin, 2002). However, these approaches are limited by their empirical nature, lacking clear quantitative criteria for selecting the data subsets used to establish  $(OC/EC)_{\text{pri}}$ . In this study, we employed the minimum R squared (MRS) method (Millet et al., 2005; Wu and Yu, 2016; Wu et al., 2018a) to determine  $(OC/EC)_{\text{pri}}$ . This method calculates a set of hypothetical  $(OC/EC)_{\text{pri}}$  and SOC values to identify the minimum correlation coefficient ( $R^2$ ) between SOC and EC, allowing for the accurate derivation of  $(OC/EC)_{\text{pri}}$ .

249

## 250 (2) Playa salt (ps) and non-playa salt (nps)

To differentiate the contributions of salt lake sources to water-soluble ions in atmospheric deposition, we adopted a methodology similar to that used for marine aerosols. This approach relies on the ratio of water-soluble ions ( $SO_4^{2-}$ ,  $Ca^{2+}$ ,  $K^+$ ,  $Mg^{2+}$ ,  $Cl^-$ ) to  $Na^+$  in the salt lakes of the QDB, enabling us to assess the contribution of ps- $Na^+$  components to nps (Zhang, 1987); details in Zhu (2025).

$$256 \quad nps-SO_4^{2-} = [SO_4^{2-}] - 0.333 \cdot ps-Na^+, \quad (4)$$

$$257 \quad nps-Ca^{2+} = [Ca^{2+}] - 0.062 \cdot ps-Na^+, \quad (5)$$

$$258 \quad nps-K^+ = [K^+] - 0.087 \cdot ps-Na^+, \quad (6)$$

$$259 \quad nps-Mg^{2+} = [Mg^{2+}] - 0.051 \cdot ps-Na^+, \quad (7)$$

$$260 \quad nps-Cl^- = [Cl^-] - 2.287 \cdot ps-Na^+, \quad (8)$$

This was accomplished using equations that incorporate total  $Na^+$ , total  $Ca^{2+}$ , the average crustal ratio  $(Na^+/Ca^{2+})_{\text{crust}} = 0.56$  w/w (Bowen, 1979), and the average  $(Ca^{2+}/Na^+)$  ratio for Qaidam salt lakes,  $(Ca^{2+}/Na^+)_{\text{salt lake}} = 0.06$  w/w (Zhang, 1987). Among these, the mass concentration of  $[SO_4^{2-}]$ ,  $[Ca^{2+}]$ ,  $[K^+]$ ,  $[Mg^{2+}]$ ,  $[Na^+]$  and  $[Cl^-]$  were identified as constituents of dust-fall.

$$265 \quad ps-Na^+ = [Na^+] - nps-Na^+, \quad (9)$$

$$266 \quad nps-Na^+ = nps-Ca^{2+} \cdot (Na^+/Ca^{2+})_{\text{crust}}, \quad (10)$$

$$267 \quad nps-Ca^{2+} = [Ca^{2+}] - ps-Ca^{2+}, \quad (11)$$

$$268 \quad ps-Ca^{2+} = ps-Na^+ \cdot (Ca^{2+}/Na^+)_{\text{salt lake}}, \quad (12)$$

269



270 (3) HYSPLIT backward trajectory model

271 Backward trajectory clustering analysis was conducted on sampling points using the TrajStat  
272 plugin within Meteoinfo software. Daily backward trajectories for 48 hours were calculated from  
273 January 2020 to March 2023 and classified monthly based on differences in the horizontal  
274 movement direction and velocity of air masses. The trajectories were initiated at Universal Time  
275 (UTC) 00:00, with a 6-hour increment, originating from 500 m above sea level (Yang et al., 2014).  
276 Meteorological data utilized in this research were obtained from the Global Data Assimilation  
277 System (GDAS) provided by the U.S. National Centers for Environmental Prediction (NCEP),  
278 covering the period from December 2019 to February 2023 (Meteoinfo software website:  
279 <http://meteothink.org>).

280

281 (4) PMF model

282 PMF is a multivariate factor analysis tool that decomposes a matrix of speciated sample data  
283 into two matrices: factor contributions (G) and factor profiles (F). The goal of PMF model is to  
284 solve the chemical mass balance between measured species concentrations and the respective source  
285 profiles, with the purpose of minimizing the object function Q (Eq. 13) based upon the uncertainties  
286 ( $u_{ij}$ ) of measured species (Paatero and Tapper, 1994).

$$287 \quad e_{ij} = x_{ij} - \sum_{h=1}^p g_{ih} f_{hj}; Q = \sum_{i=1}^m \sum_{j=1}^n (e_{ij}/h_{ij} s_{ij})^2, \quad (13)$$

288 where  $x_{ij}$  is the measured concentration of the  $j^{\text{th}}$  species in the  $i^{\text{th}}$  sample at receptor sites.  $f_{kj}$  is the  
289 source profile of the  $j^{\text{th}}$  species in the  $k^{\text{th}}$  factor and  $g_{ik}$  is the mass contribution of the  $k^{\text{th}}$  factor in  
290 the  $i^{\text{th}}$  sample.  $e_{ij}$  is the difference between modeled concentrations and measured concentrations.  
291 The uncertainty for individual species ( $u_{ij}$ ) was calculated to be  $x_{ij} \times \text{error fraction} + 1/3 \text{ MDL}$ , where  
292 MDL is the method detection limit. For data below the MDL, concentrations were replaced by  $1/2$   
293 MDL and the corresponding uncertainty was set to  $5/6 \text{ MDL}$  (Reff et al., 2007). An extended  
294 description of the PMF parameters used in this study and error estimate based on the model's Q  
295 value, displacement (DISP), and bootstrapping (BS) tests (DISP-BS) are provided in the  
296 Supplementary Information.

297

### 298 3. Results and discussion



### 3.1 Atmospheric dust deposition flux and water ions concentration

The total deposition flux (DF) in the southern QDB is  $5.41 \pm 5.33 \text{ g/m}^2\cdot 30\text{d}$ , slightly lower than that of the Lake Aibi Basin ( $3.32\text{-}23.4 \text{ g/m}^2\cdot 30\text{d}$ ) (Li et al., 2022), but higher than the surrounding areas of Akatama Salt Lake ( $2.93 \text{ g/m}^2\cdot 30\text{d}$ ) (Wang et al., 2014). Specifically, DF was  $4.67 \pm 4.96 \text{ g/m}^2\cdot 30\text{d}$  in rural and  $5.97 \pm 5.73 \text{ g/m}^2\cdot 30\text{d}$  in urban areas. During the HP, DF in rural and urban were  $4.62 \pm 4.15 \text{ g/m}^2\cdot 30\text{d}$  and  $4.95 \pm 5.25 \text{ g/m}^2\cdot 30\text{d}$ , respectively. In contrast, NHP showed increased DF values of  $4.77 \pm 4.42 \text{ g/m}^2\cdot 30\text{d}$  (rural) and  $7.66 \pm 6.09 \text{ g/m}^2\cdot 30\text{d}$  (urban) (Figure 2). Notably, Urban DF during NHP demonstrated a 54.6% increase relative to HP, while rural DF rose by 7.1% - contrasting previous findings that associated elevated DF with HP coal combustion (Cheng et al., 2009; Gao et al., 2013; Guo et al., 2010; Qi et al., 2018). We hypothesize that the increase in DF during the NHP is attributed to heightened tourism activity (May to September peaks season) in the QDB (Zhang et al., 2011), attracting approximately 17 million tourists annually, the number continues to grow. This influx likely leads to increased urban emissions, particularly in densely populated areas such as DLX and GEM (Figure S2), contributing to the elevated DF levels.

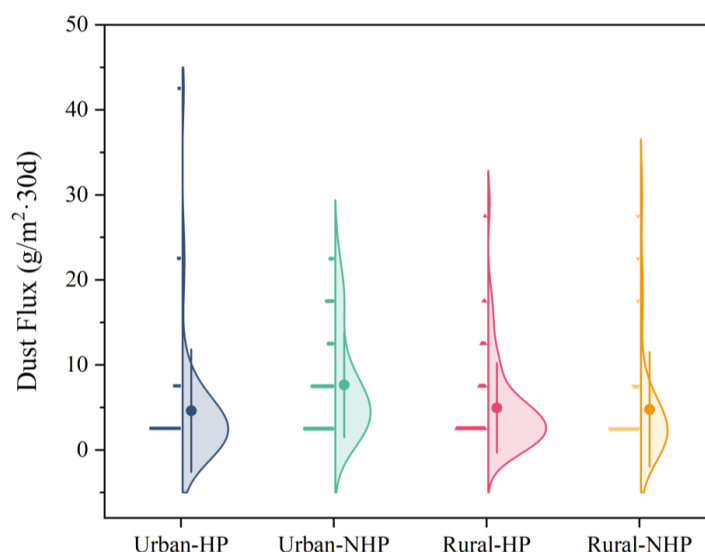


**Figure 2** Dust flux distribution in urban and rural. The distribution of dust flux in four contexts: Urban with domestic heating period (Urban-HP), Urban with non-HP (Urban-NHP), Rural with domestic heating period (Rural-HP), and Rural with non-HP (Rural-NHP). Each violin plot



318 illustrates the density distribution of dust flux values, with the central dot representing the mean,  
319 and the vertical lines indicating the interquartile range.

320

321 Water-soluble ion concentrations differed significantly between rural (115.31 mg/g) and urban  
322 (72.81 mg/g) areas. In rural, water-soluble ion content was greater during the HP than in the NHP,  
323 while the opposite trend was observed in urban areas (Figure 3, S3). We categorized the water-  
324 soluble ions in dust deposits into playa salt (ps) and non-playa salt (nps) based on their sources,  
325 following the model of marine aerosols (Zhu et al., 2025). Playa salt content consistently surpassed  
326 nps in rural areas across both periods, while urban areas showed the opposite trend. Notably, during  
327 the NHP, ps content in urban and rural increased by 54.46 and 36.86%. Backward trajectory analysis  
328 indicated that airflow in both rural and urban areas primarily originated from the northwest QDB  
329 and the eastern Tarim Basin during the HP, while during the NHP, it was influenced more broadly  
330 by the salt lake of the QDB (Figure S4, S5), aligning with the observed variations in ps content. A  
331 similar increase in summer sea salt and non-sea salt ions has been reported in Rajkot, India,  
332 attributed to ocean wind direction (Gupta and Dhir, 2022).

333 The ratio of  $\text{nps-SO}_4^{2-}/\text{NO}_3^-$  in soluble ions is used to differentiate between coal combustion  
334 (fixed sources) and vehicular emissions (mobile sources) (Arimoto et al., 1996; Shen et al., 2008).  
335 Higher ratios in urban compared to rural areas (Figure S6) suggest a greater influence of fixed  
336 sources on urban dust deposition. Additionally, the lower  $\text{nps-SO}_4^{2-}/\text{NO}_3^-$  ratio during the NHP  
337 indicates a predominant role of mobile sources in NHP dust-fall. Typically, coal and biomass  
338 burning emissions intensify during the HP in northern China (Liu et al., 2016a), while vehicle  
339 emissions dominate in the NHP (Xu et al., 2012). These findings support the validity of the analysis,  
340 however, further validation using additional indicators is recommended.

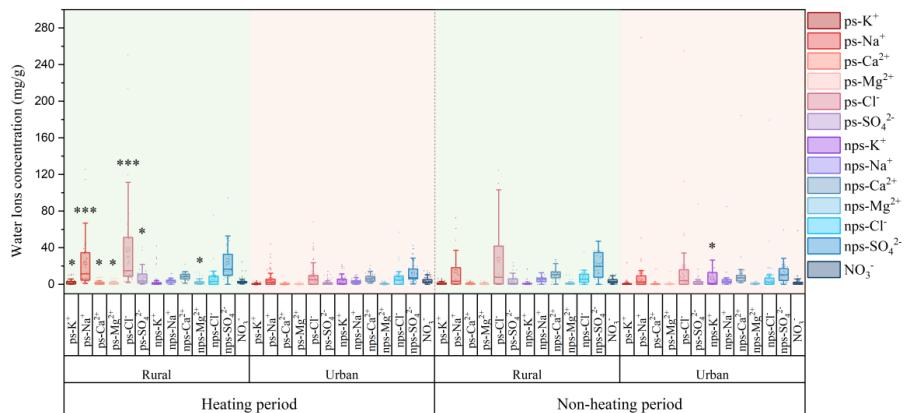


**Figure 3** Concentrations of water ions in rural and urban across different seasonal periods (domestic heating and non-domestic heating periods). Asterisks indicate statistically significant differences between sites, with \*,  $P < 0.05$ ; \*\*,  $P < 0.01$ ; \*\*\*,  $P < 0.001$ .

### 3.2 Organic carbon and element carbon compositions

The average total carbon (TC) concentration in the southern QDB was  $3.83 \pm 3.2$  mg/g, significantly lower than that of Huangshi, Hubei province ( $25.15 \pm 11.79$  mg/g) and Washington ( $157 \pm 3.2$  mg/g), Kumasi in West Africa (28 mg/g) and Xi'an ( $14.6 \pm 5.8$  mg/g) (Han et al., 2007a; Han et al., 2009b; Zhan et al., 2016; Bandowe et al., 2019), suggesting relatively low carbon emissions in the southern QDB. Average OC and EC levels in QDB are markedly lower than those in Xi'an (7.4 and 7.2 mg/g, respectively), Wuhu (33.26 and 22.49 mg/g, respectively), and Nanchang (25.15 and 11.46 mg/g, respectively) (Han et al., 2009a; Deng et al., 2014; Zhang, 2014), but significantly higher—particularly for EC—than in Nam Co (0.35 mg/g) (Chen et al., 2015).

In urban, TC content ( $3.05 \pm 2.46$  mg/g) were marginally lower than rural level ( $3.55 \pm 3.56$  mg/g), although this difference was not statistically significant. Contrasting spatial patterns emerged for carbon components: EC dominated urban areas ( $1.46 \pm 1.60$  mg/g), while OC prevailed in rural ( $2.25 \pm 1.92$  mg/g) (Figure 4, S7). This disparity may be attributed to the long-term combustion of biomass, coal, and wood in rural settings (Na et al., 2004). It may also be associated with meteorological conditions, particularly heightened solar radiation resulting from reduced primary emissions in rural areas, which facilitates the formation of SOC (Xu et al., 2018a; Wang et al., 2019).



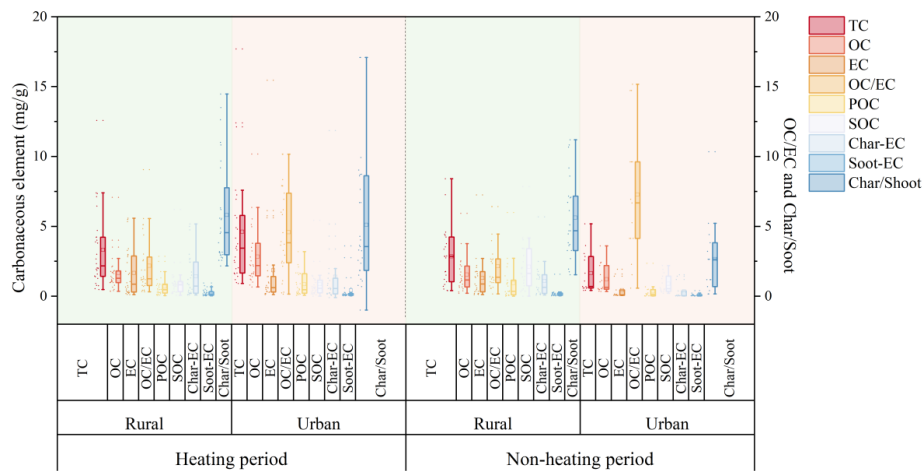


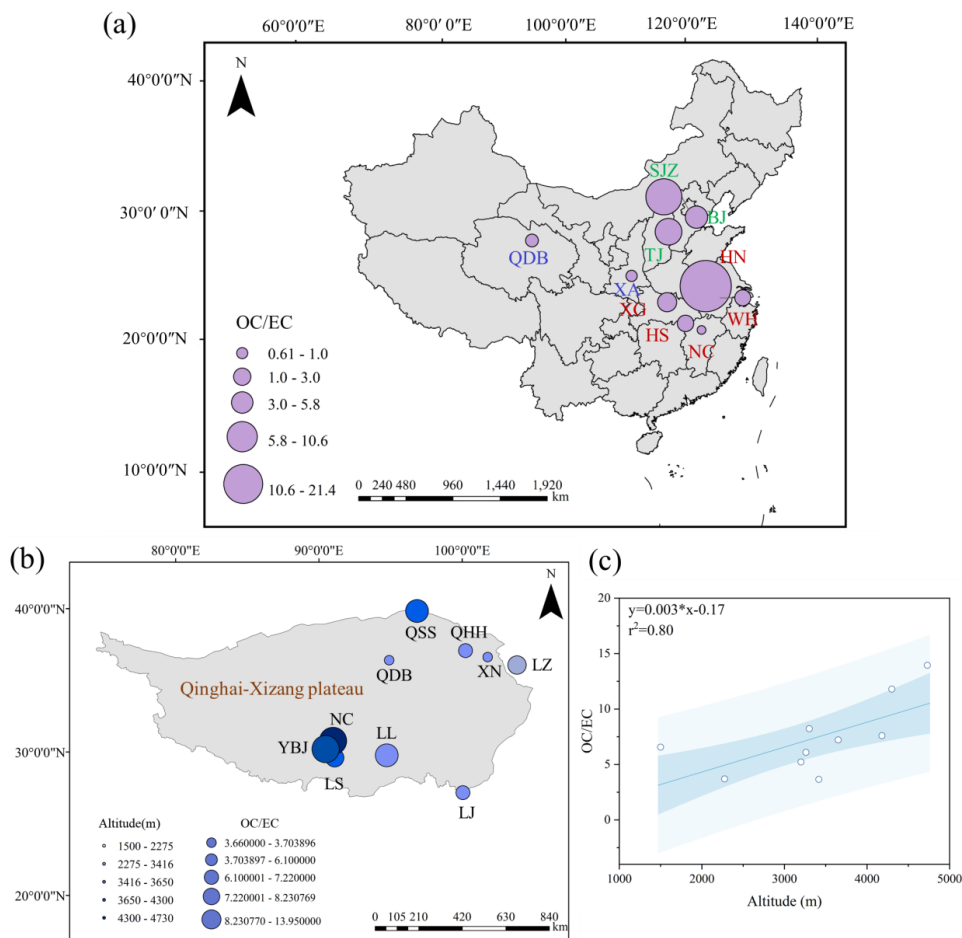
**Figure 4** Concentrations of organic carbon (OC), elements carbon (EC), secondary organic carbon (OC), primary organic carbon (POC), char-EC, soot-EC and OC/EC, char/soot ratios in different sites (Rural, Urban) and seasonal variations (domestic heating and non-domestic heating period).

Seasonal analysis revealed elevated carbonaceous compound concentrations, specifically OC and EC, during the HP. This increase is primarily due to local domestic heating activities coupled with adverse meteorological conditions, such as low temperature, weak winds (Oliveira et al., 2007; Gong et al., 2017), weak atmospheric turbulence, and frequent atmospheric inversions (Guo et al., 2016). Rural emissions primarily stem from coal and biomass burning for heating and cooking. (Zhang et al., 2000; He et al., 2004), contributing to reduced OC and EC content in the NHP, whereas elevated EC levels in urban areas are primarily linked to vehicular and industrial sources. Spatiotemporal transport dynamics show EC depletion during rural ward pollutant migration due to atmospheric dispersion, particularly affecting coarse particulate fractions.

Notably, rural carbon emissions exceed urban levels in the southern basin, potentially attributable to extended HP duration (7 months) compelling low-grade fuel (crop residues, wood, raw coal and yak dung) utilization (Na et al., 2004). In contrast, urban areas benefit from solar/wind energy infrastructure and government-led clean heating initiatives (“suitable electricity for electricity” policy), achieving 66.63% clean heating penetration (Statistical Yearbook of Haixi Xizang Autonomous Prefecture of Qinghai Province), leading to a comparatively lower TC content. The OC/EC ratio is a valuable indicator of carbonaceous aerosol sources. In this study, Urban areas



384 exhibited stable OC/EC ratios ranging from 0.15 to 15.16 (mean = 2.16), whereas rural areas showed  
385 significantly higher ratios during NHP ( $7.27 \pm 4.66$ ) compared to HP ( $4.57 \pm 3.02$ ) (Figure 4, S9).  
386 Typically, the OC/EC ratio for vehicle emissions ranges from 0.7 to 2.4, for coal combustion  
387 emissions from 0.3 to 7.6, and for biomass burning from 3.8 to 14.5 (Schmidl et al., 2008; Gonçalves  
388 et al., 2010; Pio et al., 2011; Popovicheva et al., 2016).



389  
390 **Figure 5** Distribution of OC/EC ratios across various regions of China (a), at different altitudes on  
391 the Qinghai-Xizang Plateau (b), and the relationship between OC/EC ratios and altitude (c). Blue  
392 designations represent the Northwest region, red indicates the Central region, and green denotes the  
393 Eastern region. The color of the circles corresponds to altitude, while circle size reflects the  
394 magnitude of the OC/EC ratios.



395 These findings suggest that urban OC/EC ratios (0.15-9.05) are primarily associated with  
396 vehicle and coal combustion, while rural ratios (0.14-15.16) are predominantly linked to coal and  
397 biomass burning. A higher OC/EC ratio typically indicates a greater contribution from biomass  
398 combustion; in this study, the OC/EC ratio of rural was  $5.56 \pm 3.93$ , which is significantly lower than  
399 values recorded in India (8.47) and Nam Co in Xizang ( $16.3 \pm 4.4$ ) (Saud et al., 2013; Chen et al.,  
400 2015), yet higher than those observed in Shanxi (0.7-1.6), Beijing (1.9-2.7), and Tianjin rural (2.66)  
401 (Zhang et al., 2007; Cheng et al., 2015; Wang et al., 2021). This finding indicates that  
402 carbonaceous aerosols in rural QDB derive from both fossil fuel combustion and biomass burning,  
403 suggesting source specificity.

404 Figure 5a presents spatial variations in urban OC/EC ratios across China. The findings reveal  
405 that the Northwest region, represented by QDB urban and Xi'an (XA) (Han et al., 2009b), exhibits  
406 a significantly lower ratio ( $1.59 \pm 0.56$ ) compared to central regions, including Nanchang (NC)  
407 (Zhang, 2014), Huangshi (HS) (Zhan et al., 2016), Wuhu (WH) (Deng et al. 2014), Xiaogan (XG)  
408 (Zhan et al., 2022), and Huainan (HN) (Liu et al., 2020), where the ratio is  $5.86 \pm 7.81$ . This ratio is  
409 also lower than that observed in eastern cities such as Beijing (BJ) (Tang et al., 2013), Tianjin (TJ)  
410 (Ma et al., 2019), and Shijiazhuang (SJZ) (Guo et al., 2018), which have a ratio of  $6.83 \pm 2.77$ . This  
411 pattern is consistent with the trends in atmospheric PM OC/EC ratios (Xie et al., 2023), suggesting  
412 that the carbon in the dust of the QDB urban primarily results from coal combustion and industrial  
413 emissions, leading to elevated EC concentrations and lower OC/EC ratios (Liu et al., 2022).  
414 Conversely, cities with higher economic development, such as Beijing and Tianjin, characterized by  
415 greater population density and income levels, typically experience secondary pollution, resulting in  
416 higher OC/EC ratios.

417 We analyzed the impact of altitude on the OC/EC ratio across various regions of the QXP by  
418 comparing aerosol emissions ( $PM_{2.5}$ ,  $PM_{10}$ , TSP) from several sites: QDB (this study, altitude 3416  
419 m), Lhasa (LS, altitude 3650 m) (Wei et al., 2019), Nam Co (NC, altitude 4730 m) (Chen et al.,  
420 2015; Wu et al., 2018b), Xining (XN, altitude 2275 m) (Hu et al., 2020), Qilian Shan Station of  
421 Glaciology and Ecologic Environment (QSS, altitude 4180 m) (Xu et al., 2015), Lijiang (LJ, altitude  
422 3260 m) (Zhao et al., 2019), Qinghai Lake (QHH, altitude 3200 m) (Jun Li et al., 2013; Zhang et  
423 al., 2014), Lanzhou (LZ, altitude 1500 m) (Qi et al., 2024), Yangbajing (YBJ, altitude 4300 m)  
424 (Xiang et al., 2024), and Lulang (LL, altitude 3330 m) (Li et al., 2016). The findings (Figure 5b, c)



425 demonstrated a significant positive correlation between altitude and the OC/EC ratio ( $r^2 = 0.80$ ),  
426 indicating an altitude-dependent relationship (Zhao et al., 2022). This relationship may be attributed  
427 to the limited sources of EC at higher altitudes and the predominance of aged organic aerosols,  
428 which are rich in secondary OC, leading to increased OC/EC ratios (Sandrini et al., 2014; Wu et al.,  
429 2018b). The widespread biomass burning in the QXP further contributes to the presence of semi-  
430 volatile organic carbon in aerosols, which has a lower light-absorption capacity (Kocbach Bølling  
431 et al., 2009), thereby enhancing the OC/EC ratio.

432 Both increased altitude and economic development elevate OC/EC ratio, though eastern  
433 regions exhibit lower values than high-altitude zones. High-altitude areas show depressed OC and  
434 EC concentrations overall, with ratio elevation potentially stemming from EC reduction via  
435 intensive biomass burning. Conversely, the higher ratios observed in economically developed urban  
436 are primarily driven by anthropogenic activities that facilitate the formation of SOA. These  
437 scenarios can be differentiated using the WSOC/OC ratio (Patel et al., 2022), though such analyses  
438 await experimental validation. Additionally, since this research primarily focused on PM larger than  
439  $10\ \mu\text{m}$ , the OC/EC results may be misleading. Further investigation of atmospheric particles smaller  
440 than  $10\ \mu\text{m}$  is necessary to elucidate the impact of altitude on carbonaceous aerosol emissions.

441 The elevation of QDB (3416 m) is below the average for QXP (4,000 m), and it exhibits higher  
442 economic development and population density. Despite this, some herders still burn yak dung for  
443 heating. The OC, EC emissions, and OC/EC ratios indicate that the carbon sources—comprising  
444 coal, biomass, and yak dung—are distinct from those in both central and eastern of China  
445 economically developed regions and other high-altitude QXP areas, reflecting its unique regional  
446 characteristics.

447

### 448 **3.3 Char-EC and Soot-EC compositions**

449 EC is classified into soot and char (Han et al., 2009b), with char-EC and soot-EC defined as  
450 (EC1-OPC) and (EC2+EC3), respectively (Han et al., 2007). Char-EC is typically produced from  
451 biomass burning at relatively low temperatures, whereas soot-EC originates from high-temperature  
452 coal combustion and automotive emissions (Zhu et al., 2010; Cao et al., 2013). The char-EC/soot-  
453 EC ratio, like the OC/EC ratio, serves as an indicator of carbon aerosol sources. Since char and soot



are mainly generated through combustion processes, their ratio is typically influenced by two key factors: the primary emission source and the deposition removal efficiency. For localized PM, such as in urban areas, the removal rate is generally negligible (Han et al., 2009a).

Char-EC constitutes 75.88% of rural EC (74.71% HP; 78.84% NHP) and 85.00% of urban EC (85.58% HP; 84.11% NHP) (Figure 4, S8), demonstrating its dominance across spatial and temporal scales. Research suggests that char-EC constitutes a larger proportion of coarse PM, while soot-EC is more predominant in fine particles, resulting in extended atmospheric residence times for soot-EC due to reduced deposition velocities (Han et al., 2009b). The increased levels of char-EC during the urban HP are linked to complex sources, including biomass fuel usage and transportation emissions, resulting in elevated char concentrations in urban areas and along busy roadways (Kim et al., 2011).

The char/soot ratios for automobile emissions, coal combustion, and biomass burning are 0.60, 1.9, and 11.6, respectively (Chow et al., 2004; Chuang et al., 2014). Generally, high-temperature combustion (e.g., vehicle and industrial processes) yields lower char and soot concentrations, while low-temperature combustion (e.g., household cooking and biomass burning) results in higher ratios (Han et al., 2016; Han et al., 2012; Han et al., 2010; Han et al., 2009a). Differences in char/soot ratios between urban and rural areas across seasons may be linked to wheat straw burning, contrasting with minimal vegetation combustion impacts in cities like Xi'an (Cao et al., 2005). The char/soot ratio for dust-fall observed in this study (4.97; Figure 4, S9) is slightly higher than those recorded in Jinchang (3.84) (Han et al., 2009a) and Daheihe, Inner Mongolia (3.2) (Han et al., 2008). The relatively stable concentration of soot-EC in this study, along with the elevated char/soot ratio, suggests a correlation with higher coal consumption among local residents and industries. This indicates that, in comparison to other regions, carbon emissions in the remote QDB are predominantly sourced from coal and biomass burning, supporting previous findings. Furthermore, the char/soot ratio is elevated during HP, highlighting the predominant influence of coal and biomass burning in rural areas during HP, while fossil fuel impacts are more pronounced in NHP.

### 3.4 POC and SOC compositions

Aerosol samples with low OC/EC ratios typically exhibit low concentrations of POC, which



mainly comprises primary carbonaceous compounds. Conversely, OC/EC ratios exceeding 2.0 indicate substantial SOA formation (Chow et al., 1996; Gray et al., 1986). The MSR method enables discrimination of OC into POC and SOC (Method 2.7) (Turpin and Huntzicker, 1995; Cao, 2003).

SOC constitutes a dominant fraction of OC in atmospheric aerosols. Research on carbonaceous aerosols in various Chinese cities indicates that SOC contributes 67% (53-83%) and 57% (48-62%) to rural and urban OC, respectively (Zhang et al., 2008)—marginally higher than the 62.62% observed in this study (Figure 4, S10). Although SOC formation relies on solar radiation, the QDB experiences high levels of solar energy (Liu et al., 2017), which may facilitate photochemical oxidation of VOCs into SOC (Hama et al., 2022). Nevertheless, the consistently low SOC concentrations indicate that VOCs emissions in QDB are significantly lower than the regional averages observed across China, reflecting relatively low pollution levels. This finding is consistent with the previously observed low concentrations of atmospheric carbon emission in the region.

During the NHP, rural areas exhibit the highest SOC/OC ratio of 86.70% (Figure S11), while urban areas record the lowest ratio of 44.32% during the HP. This trend reflects elevated potential for photochemical activity and reduced contributions from POC, likely due to local emission sources, such as traffic and coal combustion (Mbengue et al., 2018). The high SOC/OC ratio suggests that SOC largely displaces OC. Our findings indicate that SOC levels are greater in rural areas (66.52%) compared to urban regions (58.74%), likely attributable to significant coal consumption for domestic heating, which enhances emissions of semi-volatile organic compounds and organic gases (Dan, 2004). As for seasonal variations, studies in California show an increase in SOC levels during warmer months, which is consistent with our results (Na et al., 2004). This contrasts with the broader observation that higher temperatures typically lead to lower SOC concentrations (Strader et al., 1999; Sheehan and Bowman, 2001). This discrepancy may stem from varying sources of SOC emissions throughout the seasons, necessitating further investigation in conjunction with other carbonaceous indicators.

### 3.5 Trace elements concentration

The total concentration of major (Fe, Si, Al) and trace elements (Ti, Cr, Cd, Cu, Mn, Ni, Pb, V, Zn) was determined to be  $8.74 \pm 5.82$  mg/g, while arsenic (As) remained below the detection limit



in all analyzed samples. Crustally derived elements—Fe, Al, Si, and Ti—dominated the elemental profile, aligning with dust composition patterns reported in Ira, Singapore, and Beijing-Hebei regions, China (Joshi et al., 2009; Qiao et al., 2013; Eivazzadeh et al., 2021). In comparison to cities such as Beijing, Shanghai, Xi'an, and Lanzhou, and Junggar Basin the levels of heavy metals in dust from the QDB are relatively low (Jiang et al., 2018) (Supplementary Table S1).

Throughout both the HP and NHP, trace elements concentrations in urban areas were consistently higher than in rural areas, with the exception of Ti (Figure 6, S12). During the HP, urban levels of Zn, Pb, and Cu were significantly elevated compared to rural areas, and Pb also demonstrated a significant increase in urban during the NHP. In rural, the differences in metal concentrations between HP and NHP were minimal. In contrast, urban areas exhibited higher concentrations of all elements except for Ti, Cd, and Cr during the HP, with Fe and V showing notably elevated levels compared to other regions. These variations in average concentrations indicate that coal combustion for domestic heating in urban areas contributes to increased atmospheric heavy metal levels (Duan and Tan, 2013; Meng et al., 2017). In contrast, Cd and Cr exhibited mixed anthropogenic sources with limited coal combustion contributions, while Ti concentrations remained stable across seasons, reflecting minimal anthropogenic influence.

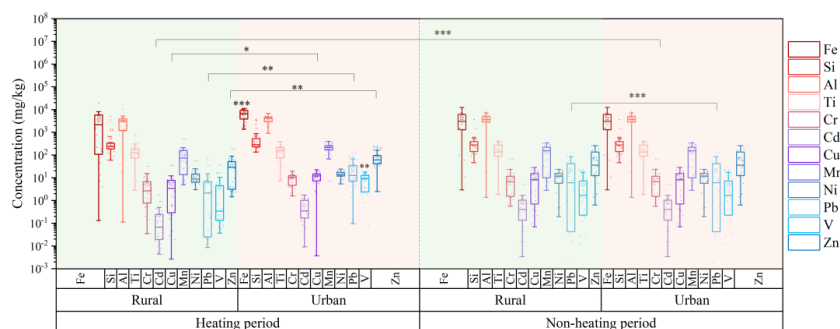


**Figure 6** Concentration of heavy metals by rural and urban settings during domestic heating and non-domestic heating periods. Significant differences are indicated by asterisks (\*p < 0.05; \*\*p < 0.01; \*\*\*p < 0.001).

### 3.6 Source apportionment

We conducted a PMF source apportionment analysis on soluble ions, trace metals, and carbonaceous elements present in dust, specifically focusing on ps-SO<sub>4</sub><sup>2-</sup>, ps-Ca<sup>2+</sup>, ps-K<sup>+</sup>, ps-Mg<sup>2+</sup>,



536  $\text{ps-Cl}^-$ ,  $\text{ps-Na}^+$ ,  $\text{nps-SO}_4^{2-}$ ,  $\text{nps-Ca}^{2+}$ ,  $\text{nps-K}^+$ ,  $\text{nps-Mg}^{2+}$ ,  $\text{nps-Cl}^-$ ,  $\text{nps-Na}^+$ , Fe, Si, Al, Ti, Cr, Cd, Cu,  
537 Mn, Ni, Pb, V, Zn, SOC, POC and Char-EC, Soot-EC. Seven source factors were identified based  
538 on prior research and an understanding of potential local sources: salt lakes, soil, vehicular  
539 emissions, secondary sources, biomass and coal burning, and industrial activities (Figure 7, S13).  
540 The factor profiles for each element in these source categories represent the arithmetic mean of  
541 profiles from six stations, with detailed operational methods provided in Supplementary Text S1.

542 The ions  $\text{ss-Na}^+$ ,  $\text{ss-Cl}^-$ ,  $\text{ss-SO}_4^{2-}$ ,  $\text{ss-Ca}^{2+}$ ,  $\text{ss-K}^+$ , and  $\text{ss-Mg}^{2+}$  are widely acknowledged as  
543 indicators of sea salt (Ambade et al., 2022; Aswini et al., 2022; Gluscic et al., 2023). In this study,  
544 we identified  $\text{ps-Cl}^-$  (82.71%),  $\text{ps-Mg}^{2+}$  (79.03%),  $\text{ps-K}^+$  (79.02%),  $\text{ps-Na}^+$  (78.69%),  $\text{ps-Ca}^{2+}$   
545 (78.70%), and  $\text{ps-SO}_4^{2-}$  (78.69%) as key markers of salt lake sources. Furthermore, Cd (29.70%)  
546 was detected at multiple sampling sites, indicating contributions from both salt lakes and industrial  
547 emissions. The contribution of salt lake sources in rural (12.93%) was significantly higher than in  
548 urban (10.33%). During the HP, the proportion of salt lake sources in rural areas was 5.49%,  
549 compared to 20.37% in the NHP; urban showed contributions of 18.24% during the HP and 2.42%  
550 in the NHP. This inverse trend suggests that seasonal variations differentially influence the  
551 contribution of salt lake sources in urban and rural, necessitating further research to elucidate the  
552 underlying driving factors.

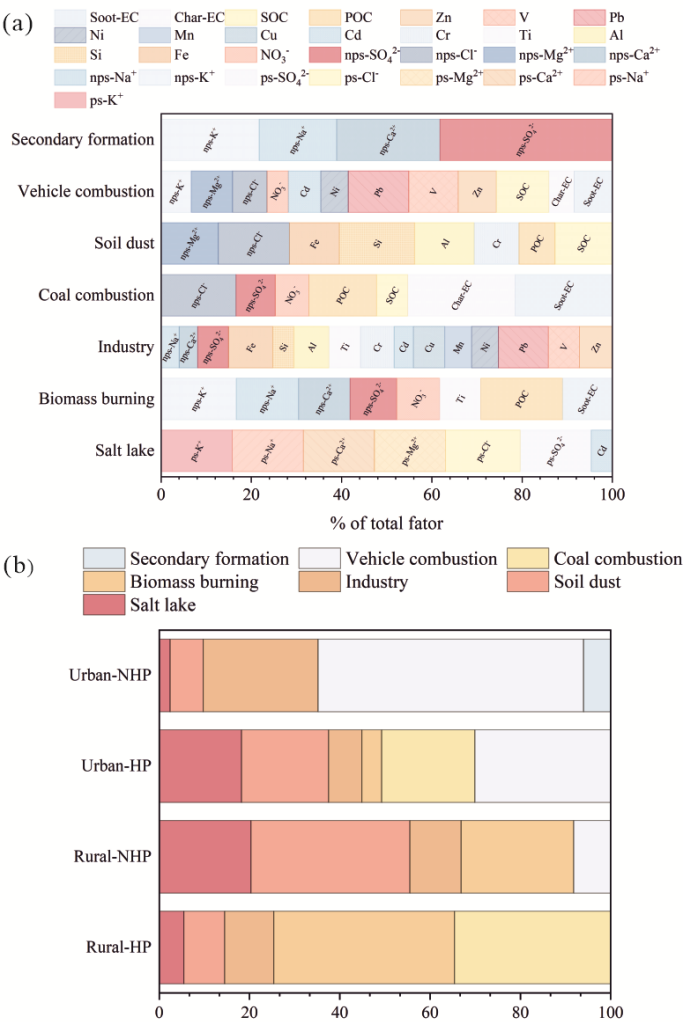
553 The second factor pertains to soil dust, characterized by ions such as Si (37.17%) and Al  
554 (29.18%), along with  $\text{nps-Cl}^-$  (34.90%),  $\text{nps-Mg}^{2+}$  (28.21%), and Fe (24.43%) (Pervez et al., 2018;  
555 Tian et al., 2021). Additionally, the proportions of elements such as SOC (28.20%) and POC  
556 (17.70%) suggest that the dust is likely mixed with fossil fuel emissions. Notably, the contribution  
557 of soil dust in rural areas (22.11%) exceeded that in urban areas (13.33%), indicating that soil dust  
558 is a major source of atmospheric deposition. In urban areas, the contribution during the NHP was  
559 relatively low (7.36%), likely due to higher wind speeds and the effectiveness of frequent summer  
560 precipitation (Zhang et al., 2015a).

561 The third factor is vehicular emissions, which are particularly pronounced in urban areas. Key  
562 characteristic elements include Pb (59.52%), V (48.73%), Zn (37.47%),  $\text{nps-Cl}^-$  (33.83%), Cd  
563 (32.43%), Ni (27.01%) and SOC (51.71%), Soot-EC (37.56%), Char-EC (24.94%) (Adeniran et al.,  
564 2017). Furthermore, notable concentrations of  $\text{nps-Mg}^{2+}$  (40.78%),  $\text{nps-K}^+$  (29.64%), and  $\text{NO}_3^-$   
565 (20.99%) were identified. In rural areas, vehicular emissions contributed 8.17% to atmospheric





566 deposition during the NHP, whereas in urban areas, the contribution was significantly higher at  
567 45.13%, with 30.07% during the HP and 58.78% in the NHP. These findings correlate with previous  
568 studies on OC/EC and char/soot ratios, suggesting that carbonaceous elements in the NHP primarily  
569 derive from vehicular emissions. The increase in vehicular emissions during the NHP may be linked  
570 to the expanding tourism industry in the QDB, particularly in cities like Golmud, which experience  
571 a rise in tourist numbers from May to September, subsequently leading to a surge in population and  
572 vehicles, and thus elevating vehicular emissions.



573  
574 **Figure 7** Factor profile and contributions in urban and rural aera. (a) presents the factor profiles,



575 represented as the arithmetic mean of individual elements across various locations, highlighting  
576 only those elements that constitute more than 20% of each profile. (b) illustrates the contributions  
577 of different sources at each location. [HP, domestic heating period; NHP, non-domestic heating  
578 period].

579

580 The fourth factor is coal combustion, characterized by high concentrations of  $\text{nps-Cl}^-$  (50.93%),  
581  $\text{nps-SO}_4^{2-}$  (26.61%),  $\text{NO}_3^-$  (22.82%), and Char-EC (73.01%), Soot-EC (65.98%), POC (46.04%),  
582 SOC (21.12%) (Kundu and Stone, 2014; Contini et al., 2016). Coal combustion occurs exclusively  
583 during the HP, contributing 34.57% in rural areas and 20.63% in urban areas. These results align  
584 with earlier studies on carbonaceous aerosols, indicating that the carbon content from coal  
585 combustion emissions is higher in rural regions than in urban environments. Consistent with  
586 northern China, air pollution in QDB urban has declined due to the adoption of clean heating  
587 technologies (Zhang et al., 2021; Xue et al., 2023). However, rural coal combustion remains a major  
588 source of carbonaceous aerosols during the HP.

589 The fifth factor, biomass burning, is characterized by significant concentrations of non-  
590 precipitating species, including  $\text{nps-K}^+$  (42.76%),  $\text{nps-Na}^+$  (35.49%),  $\text{nps-Ca}^{2+}$  (29.23%),  $\text{nps-SO}_4^{2-}$   
591 (26.56%),  $\text{NO}_3^-$  (24.46%), Ti (23.41%) and POC (46.48%), Soot-EC (28.33%) (Simoneit, 2002;  
592 Sulong et al., 2019). Biomass burning contributes 32.82% to rural atmospheric dust deposition, with  
593 a higher proportion during the HP (39.21%) compared to NHP (26.44%). In urban, biomass burning  
594 is primarily observed during the HP, contributing only 2.19%. These findings underscore biomass  
595 burning as a major source of carbon emissions in rural settings, aligning with the prevalent use of  
596 biomass fuels for cooking and domestic heating in Northern China's rural areas (Meng et al., 2019),  
597 where 70% to 80% of energy demand are fulfilled by materials such as dung cakes, firewood,  
598 charcoal, and crop residues (Tao et al., 2018; Shi et al., 2019). Furthermore, increased biomass  
599 burning is also associated with the autumn harvest period (Chen et al., 2017; Li et al., 2021).

600 The sixth factor pertains to industrial emissions, which are characterized by high  
601 concentrations of Pb (55.18%), Fe (48.91%), Cr (37.05%), Zn (36.42%), Ti (35.10%), Cu (34.91%),  
602 V (34.44%), Ni (29.69%), Mn (29.59%) and Cd (21.29%) (Almeida et al., 2015; Yao et al., 2016b).  
603 These elements were consistently detected across all sampling sites, alongside Al (38.84%),  $\text{nps-}$   
604  $\text{SO}_4^{2-}$  (34.15%), Si (23.39%) and  $\text{nps-Ca}^{2+}$  (20.48%),  $\text{nps-Na}^+$  (20.02%), which indicate potential



605 contributions from soil dust. In rural areas, industrial emissions constitute 11.10% of carbon output,  
606 with contributions of 10.86% during the HP and 11.33% during the NHP. In urban areas, industrial  
607 emissions account for 16.41% overall, with 7.37% during the HP and 25.44% in the NHP. Moreover,  
608 industrial emissions are a primary source of atmospheric dust in urban regions, particularly in the  
609 QDB, which is rich in mineral resources and hosts numerous mining enterprises, thereby  
610 significantly contributing to regional air pollution.

611 The seventh factor is secondary aerosols, primarily composed of  $\text{NO}_3^-$  (68.54%),  $\text{nps-Mg}^{2+}$   
612 (41.04%),  $\text{nps-Na}^+$  (39.01%) and  $\text{nps-Ca}^{2+}$  (30.79%) (Liu et al., 2015; Liu et al., 2016a). Research  
613 indicates that  $\text{NO}_3^-$  and  $\text{SO}_4^{2-}$  primarily result from the conversion of gaseous precursors, such as  
614  $\text{SO}_2$  and  $\text{NO}_x$ , through photochemical reactions, predominantly sourced from local and regional  
615 emission (Liu et al., 2015; Tao et al., 2013). Secondary aerosols are predominantly observed in  
616 urban areas during the NHP, where they contribute 6.00% to total aerosol sources. This increase is  
617 likely due to elevated temperatures and enhanced solar radiation during this period, which promote  
618 photochemical activity (Pandolfi et al., 2010).

619 Dust deposition sources exhibit significant seasonal and spatial variations. In the QDB, coal  
620 combustion (27.60%) and biomass burning (22.21%) dominate during HP, transitioning to vehicular  
621 emissions (33.48%), soil dust (21.27%) and industry emission (18.39%) as the primary contributor  
622 in NHP. Rural areas predominantly contribute to dust through biomass and coal burning, as well as  
623 natural sources like windblown dust and salt lake emissions. This pattern aligns with increased coal  
624 usage for winter domestic heating and heightened biomass burning for cooking and heating in rural.  
625 In urban, dust deposition is briefly influenced by anthropogenic activities, including vehicle and  
626 industrial emissions, with minimal contributions from domestic heating. Such differences can be  
627 attributed to varying economic development models, industrial and energy structures, and levels of  
628 human activity (Kataki et al., 2016).

629

### 630 **3.7 Environmental implication**

631 The source apportionment analysis using PMF model indicates that in the QDB, rural dust-fall  
632 predominantly originates from the combustion of solid fuels—including firewood, yak dung, and  
633 coal—accounting for approximately 74.61% of the total contribution. This proportion significantly



634 exceeds contributions reported for rural areas in Beijing (41%) (Hua et al., 2018), Agra (54.3%)  
635 (Agarwal et al., 2020), and Beihai, Guangxi Province (66.7%) (Zhang et al., 2019).

636 The higher contribution in this study likely reflects the local energy profile, as the sampling  
637 site in Haixi Mongol and Xizang Autonomous Prefecture, Qinghai Province, primarily relies on coal,  
638 yak dung, and firewood, constituting 58%, 23.5%, and 13% of rural energy consumption,  
639 respectively (Jiang et al., 2020; Shen et al., 2021). In contrast, solid biomass fuels, including wood  
640 and yak dung, account for over 70% of rural household energy consumption in Xizang, with yak  
641 dung alone representing 53% (Liu et al., 2008; Xiao et al., 2015). Similar patterns emerge in South  
642 and Central Asia, where biomass fuels dominate residential heating (firewood: 39%; dung: 29%)  
643 (Amacher et al., 1999; Heltberg et al., 2000; Hoeck et al., 2007; Foyssal et al., 2012; Behera et al.,  
644 2015; Kerimray et al., 2018). In northern China, rural domestic heating primarily relies on coal  
645 (46%), firewood (23.8%), and electricity (15.1%) (Tao et al., 2018), further highlighting the unique  
646 energy composition of QDB.

647 Recent studies have shown that South Asia, Central Asia, and Xizang contribute significantly  
648 to high concentrations of atmospheric PM, particularly BC, which accelerates glacier melting in the  
649 QXP (Ming et al., 2010; Xia et al., 2011; Chen et al., 2015). The QDB is recognized as a significant  
650 dust source affecting the glacier surfaces on the QXP, although it is often overlooked (Dong et al.,  
651 2014; Wei et al., 2017; Zheng et al., 2021). Compared to other dust sources, the QDB exhibits higher  
652 emissions from coal combustion, giving it a unique influence on the QXP. The organic matter and  
653 pollutants, such as polycyclic aromatic hydrocarbons (PAHs), released from household solid fuel  
654 combustion—particularly coal (98%) and dung (94%)—are substantially higher than those from  
655 firewood (Leavey et al., 2017; Secrest et al., 2017; Ye et al., 2020). Consequently, the impact of PM  
656 from coal combustion in the QDB on the QXP is significant. Specifically, the presence of BC in PM  
657 increases glacier albedo, accelerating the melting of glaciers and snow in the region (Kang et al.,  
658 2020), and impacting global freshwater resources (Huss and Hock, 2018). Additionally, BC  
659 enhances cloud condensation nuclei (CCN), ice number concentration, and cloud cover (Zhou et al.,  
660 2025), thereby influencing global climate change. Furthermore, coal combustion releases harmful  
661 emissions, including CO<sub>2</sub>, NO<sub>x</sub>, CO, SO<sub>2</sub> and sulfur trioxide (SO<sub>3</sub>) (Munawer, 2018), adversely  
662 affecting local human health and exacerbating climate warming on the QXP (Liu et al., 2006; Li et  
663 al., 2023), with broader implications for global climate. Therefore, the atmospheric pollutants



664 emission of the QDB deserves considerable attention. However, this study focuses primarily on  
665 larger particles, indicating a need for further research on the environmental impacts of carbonaceous  
666 aerosols in atmospheric PM within the QDB.

667       Beyond the unique energy structure of QDB—where coal and biomass dominate during the  
668 HP—NHP atmospheric dust primarily stems from vehicle and industrial emissions, with vehicle  
669 contributions being twice as high as in the HP. This indicates that NHP atmospheric conditions are  
670 significantly influenced by resource development and tourism. Sampling sites, such as Qarhan Salt  
671 Lake, along with GEM and LTC stations within approximately 100 km (Figure 1), suggest that salt  
672 lake resource extraction has a lower impact on regional aerosols than vehicle emissions, despite salt  
673 lakes being the primary resource. This is likely because salt lake development mainly involves solar  
674 evaporation and chemical processes like extraction and adsorption, which emit fewer pollutants  
675 compared to other mining methods (Zhen, 2010). Consequently, salt lake resource exploitation  
676 exerts a relatively minor effect on local atmospheric carbonaceous aerosol.

677       Similar salt lakes with comparable environments to QDB—such as Salar de Uyuni in Bolivia,  
678 the Atacama Salt Lake in Chile, and Ombre Muerto in Argentina—are rich in lithium resources (Li  
679 et al., 2014), making them focal points for resource development. Additionally, Salar de Uyuni, the  
680 Atacama Salt Lake, Junggar Basin, and the Great Salt Lake are renowned tourist destinations. This  
681 suggests that, in arid basin salt lakes with similar climates and intensive human activity, atmospheric  
682 carbonaceous aerosols are likely influenced by resource exploitation and tourism, especially tourism.  
683 The study’s findings can inform policy decisions regarding unexploited salt lakes in South America,  
684 such as Ombre Muerto and Salar de Uyuni. However, while QDB also hosts mineral resources such  
685 as copper, iron, and tin, this research focused on larger particles ( $>100\ \mu\text{m}$ ), which are more  
686 indicative of local sources. Given that sampling was conducted around the salt lakes, potential  
687 impacts from other mineral resource developments may have been underestimated. Further research  
688 is necessary to fully assess the environmental effects of carbonaceous aerosols in QDB atmospheric  
689 particles.

690

## 691 **Conclusion**

692       This study analyzed the composition of dust deposition at six sampling sites in the southern



693 Qaidam Basin from January 2020 to March 2023 and examined DF, soluble ion, metal, and  
694 carbonaceous element content in urban and rural samples during both domestic heating and non-  
695 domestic heating periods. Through integrated application of backward trajectory modeling, PMF,  
696 and carbon speciation indices, we identified dominant dust sources and evaluated domestic heating  
697 impacts on atmospheric processes in remote regions.

698 The findings revealed that DF and carbon emissions were significantly higher in rural than in  
699 urban areas. Among carbon indicators, urban exhibited elevated EC levels, while OC levels were  
700 higher in rural. Both altitude and economic development increase OC/EC ratios, but they are driven  
701 by different intrinsic factors. Char-EC was the dominant contributor to EC, with urban Char-EC  
702 levels showing a notable increase compared to rural levels. SOC was the principal contributor to  
703 OC, with rural SOC levels surpassing those in urban areas. The OC/EC and char-EC/soot-EC ratios,  
704 along with PMF results, indicated that during HP, dust deposition in the QDB was primarily derived  
705 from coal (28.44%) and biomass burning (22.14%), while vehicle emissions accounted for 34.19%  
706 of dust during NHP. Coal and biomass burning were the main contributors to rural dust, strongly  
707 influenced by domestic heating, whereas urban dust predominantly originated from vehicle and  
708 industrial emissions. Compared to other dust sources in the Qinghai-Xizang Plateau, coal  
709 consumption in the QDB is higher during the domestic heating period. The resulting emissions of  
710 black carbon and greenhouse gases may exacerbate glacier melting in the region, warranting  
711 increased attention. Given the distinctive carbonaceous aerosol signatures identified in the Qaidam  
712 Basin, we recommend prioritizing their radiative forcing effects in regional environmental  
713 policymaking and climate modeling frameworks. Furthermore, findings of this study offer a  
714 valuable scientific basis for understanding atmospheric carbonaceous aerosols in arid basins and  
715 salt lake regions with climates similar to QDB. They can particularly inform policy decisions  
716 regarding unexploited salt lakes in South America, such as Ombre Muerto and Salar de Uyuni.

717 However, this study primarily focused on larger-scale PM and examined the effects of heating  
718 on carbonaceous aerosols in the QDB. It lacks an investigation of aerosols with smaller particle  
719 sizes (e.g., PM<sub>10</sub>, PM<sub>2.5</sub>, PM<sub>1</sub>), which is essential for a comprehensive understanding of  
720 carbonaceous aerosol characteristics in this unique region. Furthermore, in addition to offline  
721 observations, future research should incorporate online observations with high spatiotemporal  
722 resolution and utilize numerical air quality models such as CMAQ, CAMx, WRF-CHEM, and



723 NAQPMS to analyze the spatiotemporal distribution and future trends of carbon aerosols in the  
724 QDB.

725

#### 726 **Author contribution**

727 HZ: Conceptualization, data curation, formal analysis, funding acquisition, investigation,  
728 methodology, project administration, validation, writing – original draft.

729 LZ: Data curation, formal analysis, methodology.

730 SZ: funding acquisition, validation, writing – review & edited.

731 XZ: Supervision, conceptualization, funding acquisition, writing – review & edited.

732

#### 733 **Acknowledgements**

734 This research was funded by Youth Joint Fund of Lanzhou Branch of Chinese Academy of Sciences  
735 (E4400304), and by Qinghai Provincial Innovation Platform Construction Special Program (Project  
736 No. 2024-ZJ-J03), and supported by Qinghai Provincial Key Laboratory of Geology and  
737 Environment of Salt Lakes (No. The Science and Technology Plan Project of Qinghai Province  
738 Incentive Fund 2024).

739

#### 740 **Declaration of competing interest**

741 The authors declare that there is no conflict of interest.

742

#### 743 **Data availability**

744 Datasets for this research has been uploaded in Zenodo and is available at  
745 <https://doi.org/10.5281/zenodo.14382853> (Zhu, 2024).



## Reference

- Adeniran, J. A., Yusuf, R. O., and Olajire, A. A.: Exposure to coarse and fine particulate matter at and around major intra-urban traffic intersections of Ilorin metropolis, Nigeria, *Atmospheric Environment*, 166, 383-392, 10.1016/j.atmosenv.2017.07.041, 2017.
- Agarwal, A., Satsangi, A., Lakhani, A., and Kumari, K. M.: Seasonal and spatial variability of secondary inorganic aerosols in PM<sub>2.5</sub> at Agra: Source apportionment through receptor models, *Chemosphere*, 242, 125132, <https://doi.org/10.1016/j.chemosphere.2019.125132>, 2020.
- Agarwal, T. and Bucheli, T. D.: Is black carbon a better predictor of polycyclic aromatic hydrocarbon distribution in soils than total organic carbon? *Environmental Pollution*, 159, 64-70, <https://doi.org/10.1016/j.envpol.2010.09.016>, 2011.
- Aiken, A. C., DeCarlo, P. F., Kroll, J. H., Worsnop, D. R., Huffman, J. A., Docherty, K. S., Ulbrich, I. M., Mohr, C., Kimmel, J. R., Sueper, D., Sun, Y., Zhang, Q., Trimborn, A., Northway, M., Ziemann, P. J., Canagaratna, M. R., Onasch, T. B., Alfarra, M. R., Prevot, A. S. H., Dommen, J., Duplissy, J., Metzger, A., Baltensperger, U., and Jimenez, J. L.: O/C and OM/OC ratios of primary, secondary, and ambient organic aerosols with High-Resolution Time-of-Flight Aerosol Mass Spectrometry, *Environmental Science & Technology*, 42, 4478-4485, 10.1021/es703009q, 2008.
- Almeida, S. M., Lage, J., Fernández, B., Garcia, S., Reis, M. A., and Chaves, P. C.: Chemical characterization of atmospheric particles and source apportionment in the vicinity of a steelmaking industry, *Science of The Total Environment*, 521-522, 411-420, <https://doi.org/10.1016/j.scitotenv.2015.03.112>, 2015.
- Amacher, G. S., Hyde, W. F., and Kanel, K. R.: Nepali fuelwood production and consumption: Regional and household distinctions, substitution and successful intervention, *The Journal of Development Studies*, 35, 138-163, 10.1080/00220389908422584, 1999.
- Ambade, B., Sankar, T. K., Sahu, L. K., and Dumka, U. C.: Understanding sources and composition of black carbon and PM<sub>2.5</sub> in urban environments in East India, 10.3390/urbansci6030060, 2022.
- Arimoto, R., Duce, R. A., Savoie, D. L., Prospero, J. M., Talbot, R., Cullen, J. D., Tomza, U., Lewis, N. F., and Ray, B. J.: Relationships among aerosol constituents from Asia and the North Pacific during PEM-West A, *Journal of Geophysical Research: Atmospheres*, 101, 2011-2023, <https://doi.org/10.1029/95JD01071>, 1996.
- Aswini, M. A., Tiwari, S., Singh, U., Kurian, S., Patel, A., Gunthe, S. S., and Kumar, A.: Aeolian dust





776 and sea salt in marine aerosols over the Arabian Sea during the southwest monsoon: Sources and  
777 spatial variability, *ACS Earth and Space Chemistry*, 6, 1044-1058,  
778 10.1021/acsearthspacechem.1c00400, 2022.

779 Bandowe, B. A. M., Nkansah, M. A., Leimer, S., Fischer, D., Lammel, G., and Han, Y.: Chemical (C, N,  
780 S, black carbon, soot and char) and stable carbon isotope composition of street dusts from a major  
781 West African metropolis: Implications for source apportionment and exposure, *Science of The Total*  
782 *Environment*, 655, 1468-1478, 10.1016/j.scitotenv.2018.11.089, 2019.

783 Behera, B., Rahut, D. B., Jeetendra, A., and Ali, A.: Household collection and use of biomass energy  
784 sources in South Asia, *Energy*, 85, 468-480, 10.1016/j.energy.2015.03.059, 2015.

785 Bond, T. C. and and Bergstrom, R. W.: Light absorption by carbonaceous particles: An investigative  
786 review, *Aerosol Science and Technology*, 40, 27-67, 10.1080/02786820500421521, 2006.

787 Bond, T. C., Streets, D. G., Yarber, K. F., Nelson, S. M., Woo, J.-H., and Klimont, Z.: A technology-based  
788 global inventory of black and organic carbon emissions from combustion, *Journal of Geophysical*  
789 *Research: Atmospheres*, 109, <https://doi.org/10.1029/2003JD003697>, 2004.

790 Boreddy, S. K. R., Kawamura, K., Okuzawa, K., Kanaya, Y., and Wang, Z.: Temporal and diurnal  
791 variations of carbonaceous aerosols and major ions in biomass burning influenced aerosols over Mt.  
792 Tai in the North China Plain during MTX2006, *Atmospheric Environment*, 154, 106-117,  
793 <https://doi.org/10.1016/j.atmosenv.2017.01.042>, 2017.

794 Bowen, H.-J.-M.: *Environmental chemistry of the elements*. Academic Press, 1979.

795 Cao, J.-j., Wang, Q.-y., Chow, J. C., Watson, J. G., Tie, X.-x., Shen, Z.-x., Wang, P., and An, Z.-s.: Impacts  
796 of aerosol compositions on visibility impairment in Xi'an, China, *Atmospheric Environment*, 59,  
797 559-566, 10.1016/j.atmosenv.2012.05.036, 2012a.

798 Cao, J.: Characteristics of carbonaceous aerosol in Pearl River Delta Region, China during 2001 winter  
799 period, *Atmospheric Environment*, 37, 1451-1460, 10.1016/s1352-2310(02)01002-6, 2003.

800 Cao, J. J., Shen, Z. X., Chow, J. C., Watson, J. G., Lee, S. C., Tie, X. X., Ho, K. F., Wang, G. H., and  
801 Han, Y. M.: Winter and summer PM<sub>2.5</sub> chemical compositions in fourteen Chinese cities, *Journal of*  
802 *Air Waste Manage Association*, 62, 1214-1226, 10.1080/10962247.2012.701193, 2012b.

803 Cao, J. J., Zhu, C. S., Tie, X. X., Geng, F. H., Xu, H. M., Ho, S. S. H., Wang, G. H., Han, Y. M., and Ho,  
804 K. F.: Characteristics and sources of carbonaceous aerosols from Shanghai, China, *Atmospheric*  
805 *Chemistry and Physics*, 13, 803-817, 10.5194/acp-13-803-2013, 2013.



- 806 Chen, M., Li, M.-Y., Zhou, J.-Y., Fu, R.-B., Wang, X.-F., and Shen Z.: Characteristics and source analysis  
807 of heavy metal pollution in dust in a heavy industrial area of Northwest China (in Chinese),  
808 Environmental Science and Technology, 47(02), 155-164, 10.19672/j.cnki.1003-  
809 6504.1004.23.338, 2024.
- 810 Chen, P., Kang, S., Bai, J., Sillanpää, M., and Li, C.: Yak dung combustion aerosols in the Tibetan Plateau:  
811 Chemical characteristics and influence on the local atmospheric environment, Atmospheric  
812 Research, 156, 58-66, 10.1016/j.atmosres.2015.01.001, 2015.
- 813 Chen, W., Tong, D. Q., Dan, M., Zhang, S., Zhang, X., and Pan, Y.: Typical atmospheric haze during crop  
814 harvest season in northeastern China: A case in the Changchun region, Journal of Environmental  
815 Sciences, 54, 101-113, 10.1016/j.jes.2016.03.031, 2017.
- 816 Cheng, N., Peng, L., Mu, L., Ji, H.-D., Liu, X.-F., Bai, H.-L. and Zhao, Y.-K.: Organic carbon and  
817 elemental carbon in PM<sub>10</sub> from coal spontaneous combustion zones in Shanxi (in Chinese), China  
818 Environmental Science, 2015, 35: 40-44.
- 819 Cheng, X and Lin X.: Temporal and spatial distribution characteristics of dust in Shenyang and analysis  
820 of influencing factors (in Chinese). Environmental Protection Science 35(06), 1-3 + 58,  
821 10.16803/j.cnki.issn.1004-6216.2009.06.001, 2009.
- 822 Chow, J. C., Watson, J. G., Kuhns, H., Etyemezian, V., Lowenthal, D. H., Crow, D., Kohl, S. D.,  
823 Engelbrecht, J. P., and Green, M. C.: Source profiles for industrial, mobile, and area sources in the  
824 Big Bend Regional Aerosol Visibility and Observational study, Chemosphere, 54, 185-208,  
825 10.1016/j.chemosphere.2003.07.004, 2004.
- 826 Christie, J. A., Elliott, H. E., O'Connell-Lopez, S. M. O., Perry, K., Pratt, K. A., Hallar, A. G., Hrdina,  
827 A., Murphy, J. G., Riedel, T. P., Long, R. W., Mitroo, D., Haskins, J. D., and Gaston, C. J.: Halogen  
828 production from playa dust emitted from the Great Salt Lake: Implications of the shrinking Great  
829 Salt Lake on regional air quality, ACS Earth and Space Chemistry, 9, 480-493,  
830 10.1021/acsearthspacechem.4c00258, 2025.
- 831 Chuang, M.-T., Lee, C.-T., Chou, C. C. K., Lin, N.-H., Sheu, G.-R., Wang, J.-L., Chang, S.-C., Wang, S.-  
832 H., Chi, K. H., Young, C.-Y., Huang, H., Chen, H.-W., Weng, G.-H., Lai, S.-Y., Hsu, S.-P., Chang,  
833 Y.-J., Chang, J.-H., and Wu, X.-C.: Carbonaceous aerosols in the air masses transported from  
834 Indochina to Taiwan: Long-term observation at Mt. Lulin, Atmospheric Environment, 89, 507-516,  
835 10.1016/j.atmosenv.2013.11.066, 2014.



- 836 Contini, D., Cesari, D., Conte, M., and Donato, A.: Application of PMF and CMB receptor models for  
837 the evaluation of the contribution of a large coal-fired power plant to PM<sub>10</sub> concentrations, Science  
838 of The Total Environment, 560-561, 131-140, <https://doi.org/10.1016/j.scitotenv.2016.04.031>, 2016.
- 839 Dan, M.: The characteristics of carbonaceous species and their sources in PM<sub>2.5</sub> in Beijing, Atmospheric  
840 Environment, 38, 3443-3452, [10.1016/j.atmosenv.2004.02.052](https://doi.org/10.1016/j.atmosenv.2004.02.052), 2004.
- 841 de Oliveira Alves, N., Vessoni, A. T., Quinet, A., Fortunato, R. S., Kajitani, G. S., Peixoto, M. S., Hacon,  
842 S. d. S., Artaxo, P., Saldiva, P., Menck, C. F. M., and Batistuzzo de Medeiros, S. R.: Biomass burning  
843 in the Amazon region causes DNA damage and cell death in human lung cells, Scientific Reports,  
844 7, 10937, [10.1038/s41598-017-11024-3](https://doi.org/10.1038/s41598-017-11024-3), 2017.
- 845 Deng, Y., Yang, T., Gao, Q., Yang, D., Liu, R., Wu, B., Hu, L., Liu, Y., and He, M.: Cooking with biomass  
846 fuels increased the risk for cognitive impairment and cognitive decline among the oldest-old  
847 Chinese adults (2011–2018): A prospective cohort study, Environment International, 155, 106593,  
848 <https://doi.org/10.1016/j.envint.2021.106593>, 2021.
- 849 Deng Z.-W., Fang, F. -M., Jiang, P.-L., Zhang J.-Q and Lin Y.-S.: Distribution characteristics of black  
850 carbon content in surface dust in Wuhu city (in Chinese), Journal of Anqing Normal University  
851 (Natural Science Edition), 37(01), 58-62, [10.14182/j.cnki.1001-2443.2014.01.009](https://doi.org/10.14182/j.cnki.1001-2443.2014.01.009), 2014.
- 852 Dong, Z., Qin, D., Kang, S., Ren, J., Chen, J., Cui, X., Du, Z., and Qin, X.: Physicochemical  
853 characteristics and sources of atmospheric dust deposition in snow packs on the glaciers of western  
854 Qilian Mountains, China, Tellus B: Chemical and Physical Meteorology, 66, 20956,  
855 [10.3402/tellusb.v66.20956](https://doi.org/10.3402/tellusb.v66.20956), 2014.
- 856 Duan, J. and Tan, J.: Atmospheric heavy metals and Arsenic in China: Situation, sources and control  
857 policies, Atmospheric Environment, 74, 93-101, [10.1016/j.atmosenv.2013.03.031](https://doi.org/10.1016/j.atmosenv.2013.03.031), 2013.
- 858 Eivazzadeh, M., Hassanvand, M. S., Faridi, S., and Gholampour, A.: Source apportionment and  
859 deposition of dustfall-bound trace elements around Tabriz, Iran, Environmental Science and  
860 Pollution Research International, 28, 59403-59415, [10.1007/s11356-020-12173-1](https://doi.org/10.1007/s11356-020-12173-1), 2021.
- 861 Feng, W., Guo, Z., Xiao, X., Peng, C., Shi, L., Ran, H., and Xu, W.: Atmospheric deposition as a source  
862 of cadmium and lead to soil-rice system and associated risk assessment, Ecotoxicology and  
863 Environmental Safety, 180, 160-167, <https://doi.org/10.1016/j.ecoenv.2019.04.090>, 2019.
- 864 Filonchyk, M., Yan, H., Yang, S., and Lu, X.: Detection of aerosol pollution sources during sandstorms  
865 in Northwestern China using remote sensed and model simulated data, Advances in Space Research,



- 866 61, 1035-1046, <https://doi.org/10.1016/j.asr.2017.11.037>, 2018.
- 867 Foysal, M., Hossain, M., Rubaiyat, A., Sultana, S., Uddin, M. K., Sayem, M., and Akhter, J.: Household  
868 Energy Consumption Pattern in Rural Areas of Bangladesh, *Indian Journal of Energy*, 1, 72-85,  
869 2012.
- 870 Gao, G.-S., Song, L.-M., and Ma, Z.-T.: Temporal and spatial distribution of dust-fall in Qinghai Province  
871 and analysis of its influencing factors (in Chinese), *Chinese Journal of Desert Research*, 33(04),  
872 1124-1130, 2013.
- 873 Gao, H. and Washington, R.: Arctic oscillation and the interannual variability of dust emissions from the  
874 Tarim Basin: a TOMS AI based study, *Climate Dynamics*, 35, 511-522, [10.1007/s00382-009-0687-](https://doi.org/10.1007/s00382-009-0687-4)  
875 4, 2010.
- 876 Gholampour, A., Nabizadeh, R., Hassanvand, M. S., Taghipour, H., Nazmara, S., and Mahvi, A. H.:  
877 Characterization of saline dust emission resulted from Urmia Lake drying, *Journal of Environmental*  
878 *Health Science & Engineering*, 13, 82, [10.1186/s40201-015-0238-3](https://doi.org/10.1186/s40201-015-0238-3), 2015.
- 879 Gluscic, V., Zuzul, S., Pehnec, G., Jakovljevic, I., Smoljo, I., Godec, R., Beslic, I., Milinkovic, A.,  
880 Alempijevic, S. B., and Frka, S.: Sources, ionic composition and acidic properties of bulk and wet  
881 atmospheric deposition in the Eastern Middle Adriatic region, *toxics*, 11, [10.3390/toxics11070551](https://doi.org/10.3390/toxics11070551),  
882 2023.
- 883 Gonçalves, C., Alves, C., Evtyugina, M., Mirante, F., Pio, C., Caseiro, A., Schmidl, C., Bauer, H., and  
884 Carvalho, F.: Characterisation of PM<sub>10</sub> emissions from woodstove combustion of common woods  
885 grown in Portugal, *Atmospheric Environment*, 44, 4474-4480, [https://doi.org/10.1016/j.atmosenv.](https://doi.org/10.1016/j.atmosenv.2010.09.041)  
886 2010.
- 887 Gong, M., Yin, S., Gu, X., Xu, Y., Jiang, N., and Zhang, R.: Refined 2013-based vehicle emission  
888 inventory and its spatial and temporal characteristics in Zhengzhou, China, *Science of The Total*  
889 *Environment*, 599-600, 1149-1159, <https://doi.org/10.1016/j.scitotenv.2017.03.299>, 2017.
- 890 Gray, H. A., Cass, G. R., Huntzicker, J. J., Heyerdahl, E. K., and Rau, J. A.: Characteristics of atmospheric  
891 organic and elemental carbon particle concentrations in Los Angeles, *Environmental Science &*  
892 *Technology*, 20, 580-589, [10.1021/es00148a006](https://doi.org/10.1021/es00148a006), 1986.
- 893 Guo, J., Miao, Y., Zhang, Y., Liu, H., Li, Z., Zhang, W., He, J., Lou, M., Yan, Y., Bian, L., and Zhai, P.:  
894 The climatology of planetary boundary layer height in China derived from radiosonde and  
895 reanalysis data, *Atmospheric Chemistry and Physics*, 16, 13309-13319, [10.5194/acp-16-13309-2016](https://doi.org/10.5194/acp-16-13309-2016),



- 896 2016.
- 897 Guo, S., Wang, L., Zhou, P., Guo, S., Qin, W., An, S., Xiao, J.-Y., Liu, J., and Ji, Y.: Characteristics and  
898 sources of organic carbon and elemental carbon in summer road dust in Shijiazhuang (in Chinese),  
899 Environmental Engineering, 36(04), 122-126, 10.13205/j.hjgc.201804025, 2018.
- 900 Guo, W.-T., Zhao, F.-Q., and Chang, H.-L.: Analysis of the trend of environmental air quality changes in  
901 the main urban area of Changzhi City (in Chinese), Proceedings of Shanghai, China 3, 2010.
- 902 Gupta, A. and Dhir, A.: Assessment of air quality and chemical fingerprints for atmospheric fine aerosols  
903 in an Indian smart city, Environmental Pollutants and Bioavailability, 34, 21-33,  
904 10.1080/26395940.2021.2024091, 2022.
- 905 Hahnenberger, M. and Nicoll, K.: Meteorological characteristics of dust storm events in the eastern Great  
906 Basin of Utah, U.S.A, Atmospheric Environment, 60, 601-612, <https://doi.org/10.1016/j.atmosenv>,  
907 2012.
- 908 Hallquist, M., Wenger, J. C., Baltensperger, U., Rudich, Y., Simpson, D., Claeys, M., Dommen, J.,  
909 Donahue, N. M., George, C., Goldstein, A. H., Hamilton, J. F., Herrmann, H., Hoffmann, T., Iinuma,  
910 Y., Jang, M., Jenkin, M. E., Jimenez, J. L., Kiendler-Scharr, A., Maenhaut, W., McFiggans, G.,  
911 Mentel, T. F., Monod, A., Prévôt, A. S. H., Seinfeld, J. H., Surratt, J. D., Szmigielski, R., and Wildt,  
912 J.: The formation, properties and impact of secondary organic aerosol: current and emerging issues,  
913 Atmospheric Chemistry and Physics, 9, 5155-5236, 10.5194/acp-9-5155-2009, 2009.
- 914 Hama, S., Ouchen, I., Wyche, K. P., Cordell, R. L., and Monks, P. S.: Carbonaceous aerosols in five  
915 European cities: Insights into primary emissions and secondary particle formation, Atmospheric  
916 Research, 274, 10.1016/j.atmosres, 2022.
- 917 Han, Y., Cao, J., An, Z., Chow, J. C., Watson, J. G., Jin, Z., Fung, K., and Liu, S.: Evaluation of the  
918 thermal/optical reflectance method for quantification of elemental carbon in sediments,  
919 Chemosphere, 69, 526-533, 10.1016/j.chemosphere, 2007a.
- 920 Han, Y., Cao, J., Chow, J. C., Watson, J. G., An, Z., Jin, Z., Fung, K., and Liu, S.: Evaluation of the  
921 thermal/optical reflectance method for discrimination between char- and soot-EC, Chemosphere,  
922 69, 569-574, 10.1016/j.chemosphere, 2007b.
- 923 Han, Y. M., Lee, S. C., Cao, J. J., Ho, K. F., and An, Z. S.: Spatial distribution and seasonal variation of  
924 char-EC and soot-EC in the atmosphere over China, Atmospheric Environment, 43, 6066-6073,  
925 10.1016/j.atmosenv, 2009a.



- 926 Han, Y. M., Cao, J. J., Chow, J. C., Watson, J. G., An, Z. S., and Liu, S. X.: Elemental carbon in urban  
927 soils and road dusts in Xi'an, China and its implication for air pollution, *Atmospheric Environment*,  
928 43, 2464-2470, 10.1016/j.atmosenv, 2009b.
- 929 Han, Y. M., Han, Z. W., Cao, J. J., Chow, J. C., Watson, J. G., An, Z. S., Liu, S. X., and Zhang, R. J.:  
930 Distribution and origin of carbonaceous aerosol over a rural high-mountain lake area, Northern  
931 China and its transport significance, *Atmospheric Environment*, 42, 2405-2414, 10.1016/j.atmosenv,  
932 2008.
- 933 Han, Y. M., Chen, L. W. A., Huang, R. J., Chow, J. C., Watson, J. G., Ni, H. Y., Liu, S. X., Fung, K. K.,  
934 Shen, Z. X., Wei, C., Wang, Q. Y., Tian, J., Zhao, Z. Z., Prévôt, A. S. H., and Cao, J. J.: Carbonaceous  
935 aerosols in megacity Xi'an, China: Implications of thermal/optical protocols comparison,  
936 *Atmospheric Environment*, 132, 58-68, 10.1016/j.atmosenv, 2016.
- 937 He, L.-Y., Hu, M., Huang, X.-F., Yu, B.-D., Zhang, Y.-H., and Liu, D.-Q.: Measurement of emissions of  
938 fine particulate organic matter from Chinese cooking, *Atmospheric Environment*, 38, 6557-6564,  
939 10.1016/j.atmosenv, 2004.
- 940 Heltberg, R., Arndt, T. C., and Sekhar, N. U.: Fuelwood consumption and forest degradation: A household  
941 model for domestic energy substitution in rural India, *Land Economics*, 76, 213-232,  
942 10.2307/3147225, 2000.
- 943 Hoeck, T., Droux, R., Breu, T., Hurni, H., and Maselli, D.: Rural energy consumption and land  
944 degradation in a post-Soviet setting – an example from the west Pamir mountains in Tajikistan,  
945 *Energy for Sustainable Development*, 11, 48-57, [https://doi.org/10.1016/S0973-0826\(08\)60563-3](https://doi.org/10.1016/S0973-0826(08)60563-3),  
946 2007.
- 947 Hu, X., Yin, Y., Duan, L., Wang, H., Song, W., and Xiu, G.: Temporal and spatial variation of PM<sub>2.5</sub> in  
948 Xining, Northeast of the Qinghai–Xizang (Tibet) Plateau, 10.3390/atmos11090953, 2020.
- 949 Hu, Y.-N and Liu, Y.-L.: Characteristics and source analysis of heavy metal pollution in indoor dust in  
950 Jinan (in Chinese). *Environmental Science and Technology* 45(06), 179-184, 10.19672/j.cnki.1003-  
951 6504.0043.22.338, 2022.
- 952 Hua, Y., Wang, S., Jiang, J., Zhou, W., Xu, Q., Li, X., Liu, B., Zhang, D., and Zheng, M.: Characteristics  
953 and sources of aerosol pollution at a polluted rural site southwest in Beijing, China, *Science of The*  
954 *Total Environment*, 626, 519-527, <https://doi.org/10.1016/j.scitotenv>, 2018.
- 955 Huss, M. and Hock, R. Global-scale hydrological response to future glacier mass loss. *Nature Climate*



- 956 Change 8(2), 135-140, 2018.
- 957 Jiang, L., Xue, B., Xing, R., Chen, X., Song, L., Wang, Y., Coffman, D. M., and Mi, Z.: Rural household  
958 energy consumption of farmers and herders in the Qinghai-Tibet Plateau, *Energy*, 192,  
959 10.1016/j.energy.2019.116649, 2020.
- 960 Jiang, Y., Shi, L., Guang, A. I., Mu, Z., Zhan, H., and Wu, Y.: Contamination levels and human health  
961 risk assessment of toxic heavy metals in street dust in an industrial city in Northwest China,  
962 *Environmental Geochemistry and Health*, 40, 2007-2020, 10.1007/s10653-017-0028-1, 2018.
- 963 Joshi, U. M., Vijayaraghavan, K., and Balasubramanian, R.: Elemental composition of urban street dusts  
964 and their dissolution characteristics in various aqueous media, *Chemosphere*, 77, 526-533,  
965 10.1016/j.chemosphere, 2009.
- 966 Jun Li, J., Ge, H. W., Xin, M. W., Jun, J. C., Tao, S., Chun, L. C., Jing, J. M., A., F. H. T., and and Xin  
967 Liu, s.: Abundance, composition and source of atmospheric PM<sub>2.5</sub> at a remote site in the Tibetan  
968 Plateau, China, *Tellus B: Chemical and Physical Meteorology*, 65, 20281,  
969 10.3402/tellusb.v65i0.20281, 2013.
- 970 Kang, S., Zhang, Y., Qian, Y., and Wang, H.: A review of black carbon in snow and ice and its impact on  
971 the cryosphere, *Earth-Science Reviews*, 210, 10.1016/j.earscirev.2020.103346, 2020.
- 972 Kataki, R., Goswami, K., Bordoloi, N. J., Narzari, R., Saikia, R., Sut, D., and Gogoi, L.: Biomass  
973 resources for biofuel production in Northeast India, in: *Bioprospecting of indigenous bioresources*  
974 of North-East India, edited by: Purkayastha, J., Springer Singapore, Singapore, 127-151,  
975 10.1007/978-981-10-0620-3\_8, 2016.
- 976 Kerimray, A., Suleimenov, B., De Miglio, R., Rojas-Solórzano, L., Amouei Torkmahalleh, M., and Ó  
977 Gallachóir, B. P.: Investigating the energy transition to a coal free residential sector in Kazakhstan  
978 using a regionally disaggregated energy systems model, *Journal of Cleaner Production*, 196, 1532-  
979 1548, <https://doi.org/10.1016/j.jclepro>, 2018.
- 980 Kim, K. H., Sekiguchi, K., Kudo, S., and Sakamoto, K.: Characteristics of atmospheric elemental carbon  
981 (Char and Soot) in ultrafine and fine particles in a roadside environment, Japan, *Aerosol and Air*  
982 *Quality Research*, 11, 1-12, 10.4209/aaqr.2010.07.0061, 2011.
- 983 Kocbach Bölling, A., Pagels, J., Yttri, K. E., Barregard, L., Sallsten, G., Schwarze, P. E., and Boman, C.:  
984 Health effects of residential wood smoke particles: the importance of combustion conditions and  
985 physicochemical particle properties, *Particle and Fibre Toxicology*, 6, 29, 10.1186/1743-8977-6-29,



- 986           2009.
- 987   Kundu, S. and Stone, E. A.: Composition and sources of fine particulate matter across urban and rural  
988           sites in the Midwestern United States, *Environmental Science: Processes and Impacts*, 16, 1360-  
989           1370, 10.1039/c3em00719g, 2014.
- 990   Lai, S., Zhao, Y., Ding, A., Zhang, Y., Song, T., Zheng, J., Ho, K. F., Lee, S.-c., and Zhong, L.:  
991           Characterization of PM<sub>2.5</sub> and the major chemical components during a 1-year campaign in rural  
992           Guangzhou, Southern China, *Atmospheric Research*, 167, 208-215, 10.1016/j.atmosres, 2016.
- 993   Leavey, A., Patel, S., Martinez, R., Mitroo, D., Fortenberry, C., Walker, M., Williams, B., and Biswas, P.:  
994           Organic and inorganic speciation of particulate matter formed during different combustion phases  
995           in an improved cookstove, *Environmental Research*, 158, 33-42, 10.1016/j.envres, 2017.
- 996   Li, C., Kang, S., Yan, F., Zhang, C., Yang, J. and He, C.: Importance of precipitation and dust storms in  
997           regulating black carbon deposition on remote Himalayan glaciers. *Environmental Pollution* 318,  
998           120885, 2023.
- 999   Li, C., Yan, F., Kang, S., Chen, P., Hu, Z., Gao, S., Qu, B., and Sillanpää, M.: Light absorption  
1000           characteristics of carbonaceous aerosols in two remote stations of the southern fringe of the Tibetan  
1001           Plateau, China, *Atmospheric Environment*, 143, 79-85, <https://doi.org/10.1016/j.atmosenv>, 2016.
- 1002   Li, J.-K., Liu, X.-F. and Wang, D.-H.: Overview of mineralization laws of lithium deposits in China (in  
1003           Chinese). *Acta Geologica Sinica*, 88: 2269-2283. DOI: 10.19762/j.cnki.dizhixuebao, 2014.
- 1004   Li, Q.-L and Sha, Z.-J.: Remote sensing monitoring of ecological environment quality in the Qaidam  
1005           Basin under climate warming (in Chinese), *Ecological Science*, 41(06), 92-99,  
1006           10.14108/j.cnki.1008-8873, 2022.
- 1007   Li, Y., Ma, L., Ge, Y., and Abuduwaili, J.: Health risk of heavy metal exposure from dustfall and source  
1008           apportionment with the PCA-MLR model: A case study in the Ebinur Lake Basin, China,  
1009           *Atmospheric Environment*, 272, 118950, <https://doi.org/10.1016/j.atmosenv>, 2022.
- 1010   Li, Z., Yue, Z., Yang, D., Wang, L., Wang, X., Li, Z., Wang, Y., Chen, L., Guo, S., Yao, J., Lou, X., Xu,  
1011           X., and Wei, J.: Levels, chemical compositions, and sources of PM<sub>2.5</sub> of rural and urban area under  
1012           the impact of wheat harvest, *Aerosol and Air Quality Research*, 21, 10.4209/aaqr.210026, 2021.
- 1013   Lim, H.-J. and Turpin, B. J.: Origins of primary and secondary organic aerosol in Atlanta: Results of  
1014           time-resolved measurements during the Atlanta supersite experiment, *Environmental Science &*  
1015           *Technology*, 36, 4489-4496, 10.1021/es0206487, 2002.





- 1016 Liu, B., Song, N., Dai, Q., Mei, R., Sui, B., Bi, X., and Feng, Y.: Chemical composition and source  
1017 apportionment of ambient PM<sub>2.5</sub> during the non-heating period in Taian, China, *Atmospheric*  
1018 *Research*, 170, 23-33, 10.1016/j.atmosres, 2016a.
- 1019 Liu, G., Lucas, M., and Shen, L.: Rural household energy consumption and its impacts on eco-  
1020 environment in Tibet: Taking Taktse county as an example, *Renewable and Sustainable Energy*  
1021 *Reviews*, 12, 1890-1908, <https://doi.org/10.1016/j.rser, 2008>.
- 1022 Liu, G., Li, J., Wu, D., and Xu, H.: Chemical composition and source apportionment of the ambient PM<sub>2.5</sub>  
1023 in Hangzhou, China, *Particuology*, 18, 135-143, <https://doi.org/10.1016/j.partic, 2015>.
- 1024 Liu, G., Yin, G., Kurban, A., Aishan, T., and You, H.: Spatiotemporal dynamics of land cover and their  
1025 impacts on potential dust source regions in the Tarim Basin, NW China, *Environmental Earth*  
1026 *Sciences*, 75, 1477, 10.1007/s12665-016-6269-y, 2016b.
- 1027 Liu, H., Hu, B., Zhang, L., Zhao, X. J., Shang, K. Z., Wang, Y. S., and Wang, J.: Ultraviolet radiation  
1028 over China: Spatial distribution and trends, *Renewable and Sustainable Energy Reviews*, 76, 1371-  
1029 1383, <https://doi.org/10.1016/j.rser, 2017>.
- 1030 Liu, P., Zhou, H., Chun, X., Wan, Z., Liu, T., Sun, B., Wang, J., and Zhang, W.: Characteristics of fine  
1031 carbonaceous aerosols in Wuhai, a resource-based city in Northern China: Insights from energy  
1032 efficiency and population density, *Environmental Pollution*, 292, 118368,  
1033 <https://doi.org/10.1016/j.envpol, 2022>.
- 1034 Liu, S., Xia, X., Zhai, Y., Wang, R., Liu, T., and Zhang, S.: Black carbon (BC) in urban and surrounding  
1035 rural soils of Beijing, China: Spatial distribution and relationship with polycyclic aromatic  
1036 hydrocarbons (PAHs), *Chemosphere*, 82, 223-228, <https://doi.org/10.1016/j.chemosphere, 2011>.
- 1037 Liu, Y., Liu, G., Yousaf, B., Zhang, J., and Zhou, L.: Carbon fractionation and stable carbon isotopic  
1038 fingerprint of road dusts near coal power plant with emphases on coal-related source apportionment,  
1039 *Ecotoxicology and Environmental Safety*, 202, 110888, <https://doi.org/10.1016/j.ecoenv, 2020a>.
- 1040 Liu, Y., Wu, G., Duan, A and Zhang, Q.: New evidence that climate warming in the Tibetan Plateau is a  
1041 result of intensified greenhouse gas emissions (in Chinese), *Chinese Science Bulletin*, 51(8), 989-  
1042 992, 10.1360/csb2006-51-8-989, 2006.
- 1043 Liu, Y., Zhu, Q., Huang, J., Hua, S., and Jia, R.: Impact of dust-polluted convective clouds over the  
1044 Tibetan Plateau on downstream precipitation, *Atmospheric Environment*, 209, 67-77,  
1045 <https://doi.org/10.1016/j.atmosenv, 2019>.



- 1046 Liu, Y., Zhu, Q., Hua, S., Alam, K., Dai, T., and Cheng, Y.: Tibetan Plateau driven impact of Taklimakan  
1047 dust on northern rainfall, *Atmospheric Environment*, 234, 117583,  
1048 <https://doi.org/10.1016/j.atmosenv.2020b>.
- 1049 Lonati, G., Ozgen, S., and Giugliano, M.: Primary and secondary carbonaceous species in PM<sub>2.5</sub> samples  
1050 in Milan (Italy), *Atmospheric Environment*, 41, 4599-4610, [https://doi.org/10.1016/j.atmosenv](https://doi.org/10.1016/j.atmosenv.2007),  
1051 2007.
- 1052 Löw, F., Navratil, P., Kotte, K., Schöler, H. F., and Bubenzer, O.: Remote-sensing-based analysis of  
1053 landscape change in the desiccated seabed of the Aral Sea—a potential tool for assessing the hazard  
1054 degree of dust and salt storms, *Environmental Monitoring and Assessment*, 185, 8303-8319,  
1055 [10.1007/s10661-013-3174-7](https://doi.org/10.1007/s10661-013-3174-7), 2013.
- 1056 Luo, M., Liu, Y., Zhu, Q., Tang, Y., and Alam, K.: Role and mechanisms of black carbon affecting water  
1057 vapor transport to Tibet, *10.3390/rs12020231*, 2020.
- 1058 Ma, Y., Ji, Y.-Q., Guo, J.-J., Zhao, J.-Q., Li, Y.-Y., Wang, S.-B and Zhang L.: Characteristics of carbon  
1059 components and source analysis of road dust during spring in Tianjin (in Chinese), *Acta Scientiae*  
1060 *Circumstantiae* 40(06), 2540-2545, [10.13227/j.hjxk.2019](https://doi.org/10.13227/j.hjxk.2019).
- 1061 Mbengue, S., Fusek, M., Schwarz, J., Vodička, P., Šmejkalová, A. H., and Holoubek, I.: Four years of  
1062 highly time resolved measurements of elemental and organic carbon at a rural background site in  
1063 Central Europe, *Atmospheric Environment*, 182, 335-346, [10.1016/j.atmosenv.2018](https://doi.org/10.1016/j.atmosenv.2018).
- 1064 Meng, J.-H., Shi, X.-F., Xiang, Y and Ren, Y.-F.: Current status and sources of heavy metal pollution in  
1065 the atmosphere (in Chinese). *Environmental Science and Management* 42(08), 51-53, 2017.
- 1066 Meng, W., Zhong, Q., Chen, Y., Shen, H., Yun, X., Smith, K. R., Li, B., Liu, J., Wang, X., Ma, J., Cheng,  
1067 H., Zeng, E. Y., Guan, D., Russell, A. G., and Tao, S.: Energy and air pollution benefits of household  
1068 fuel policies in northern China, *Proceedings of the National Academy of Sciences*, 116, 16773-  
1069 16780, [10.1073/pnas.1904182116](https://doi.org/10.1073/pnas.1904182116), 2019.
- 1070 Meng, W., Shen, H., Yun, X., Chen, Y., Zhong, Q., Zhang, W., Yu, X., Xu, H., Ren, Y. a., Shen, G., Ma,  
1071 J., Liu, J., Cheng, H., Wang, X., Zhu, D., and Tao, S.: Differentiated-Rate Clean Heating Strategy  
1072 with Superior Environmental and Health Benefits in Northern China, *Environmental Science &*  
1073 *Technology*, 54, 13458-13466, [10.1021/acs.est.0c04019](https://doi.org/10.1021/acs.est.0c04019), 2020.
- 1074 Miller, M. B., Fine, R., Pierce, A. M., and Gustin, M. S.: Identifying sources of ozone to three rural  
1075 locations in Nevada, USA, using ancillary gas pollutants, aerosol chemistry, and mercury, *Science*



- 1076 of The Total Environment, 530-531, 483-492, <https://doi.org/10.1016/j.scitotenv>, 2015.
- 1077 Millet, D. B., Donahue, N. M., Pandis, S. N., Polidori, A., Stanier, C. O., Turpin, B. J., and Goldstein, A.
- 1078 H.: Atmospheric volatile organic compound measurements during the Pittsburgh Air Quality Study:
- 1079 Results, interpretation, and quantification of primary and secondary contributions, *Journal of*
- 1080 *Geophysical Research: Atmospheres*, 110, <https://doi.org/10.1029/2004JD004601>, 2005.
- 1081 Ming, J., Xiao, C., Sun, J., Kang, S., and Bonasoni, P.: Carbonaceous particles in the atmosphere and
- 1082 precipitation of the Nam Co region, central Tibet, *Journal of Environmental Sciences*, 22, 1748-
- 1083 1756, [https://doi.org/10.1016/S1001-0742\(09\)60315-6](https://doi.org/10.1016/S1001-0742(09)60315-6), 2010.
- 1084 Moravek, A., Murphy, J. G., Hrdina, A., Lin, J. C., Pennell, C., Franchin, A., Middlebrook, A. M., Fibiger,
- 1085 D. L., Womack, C. C., McDuffie, E. E., Martin, R., Moore, K., Baasandorj, M., and Brown, S. S.:
- 1086 Wintertime spatial distribution of ammonia and its emission sources in the Great Salt Lake region,
- 1087 *Atmospheric Chemistry and Physics*, 19, 15691-15709, [10.5194/acp-19-15691-2019](https://doi.org/10.5194/acp-19-15691-2019), 2019.
- 1088 Munawer, M. E.: Human health and environmental impacts of coal combustion and post-combustion
- 1089 wastes, *Journal of Sustainable Mining*, 17, 87-96, <https://doi.org/10.1016/j.jsm>, 2018.
- 1090 Na, K., Sawant, A. A., Song, C., and Cocker, D. R.: Primary and secondary carbonaceous species in the
- 1091 atmosphere of Western Riverside County, California, *Atmospheric Environment*, 38, 1345-1355,
- 1092 [10.1016/j.atmosenv](https://doi.org/10.1016/j.atmosenv), 2004.
- 1093 Qi, D.-L., Zhao, Q.-N., Zhao, H.-F., Han, T.-F and Su, W.-J.: Temporal and spatial characteristics and
- 1094 regional differences of dust-fall in Qinghai Province from 2004 to 2017 (in Chinese), *Arid*
- 1095 *Meteorology*, 36(06), 927-935, 2018.
- 1096 Qian, G.-Q and Dong, Z.-B.: Research on methods and related issues of atmospheric dust collection (in
- 1097 Chinese), *Chinese Journal of Desert Research*, (06), 119-122, 2014.
- 1098 Oliveira, T., Pio, C., Alves, C., Silvestre, A., Evtyugina, M., Afonso, J., Caseiro, A., and Legrand, M.:
- 1099 Air quality and organic compounds in aerosols from a coastal rural area in the Western Iberian
- 1100 Peninsula over a year long period: Characterisation, loads and seasonal trends, *Atmospheric*
- 1101 *Environment*, 41, 3631-3643, [10.1016/j.atmosenv](https://doi.org/10.1016/j.atmosenv), 2007.
- 1102 Paatero, P. and Tapper, U.: Positive matrix factorization: A non-negative factor model with optimal
- 1103 utilization of error estimates of data values, *Environmetrics*, 5, 111-126,
- 1104 <https://doi.org/10.1002/env.3170050203>, 1994.
- 1105 Pandolfi, M., Gonzalez-Castanedo, Y., Alastuey, A., de la Rosa, J. D., Mantilla, E., de la Campa, A. S.,



- 1106 Querol, X., Pey, J., Amato, F., and Moreno, T.: Source apportionment of PM<sub>10</sub> and PM<sub>2.5</sub> at multiple  
1107 sites in the strait of Gibraltar by PMF: impact of shipping emissions, *Environmental Science and*  
1108 *Pollution Research*, 18, 260-269, 10.1007/s11356-010-0373-4, 2010.
- 1109 Pani, S. K., Wang, S.-H., Lin, N.-H., Tsay, S.-C., Lolli, S., Chuang, M.-T., Lee, C.-T., Chantara, S., and  
1110 Yu, J.-Y.: Assessment of aerosol optical property and radiative effect for the layer decoupling cases  
1111 over the northern South China Sea during the 7-SEAS/Dongsha Experiment, *Journal of Geophysical*  
1112 *Research: Atmospheres*, 121, 4894-4906, <https://doi.org/10.1002/2015JD024601>, 2016.
- 1113 Patel, A., Rastogi, N., Rangu, S., Dave, J., Borgohain, A., and Kundu, S. S.: Oxidative potential and  
1114 hydroxyl radical generation capacity of ambient PM<sub>2.5</sub> over a high-altitude site in northeastern  
1115 Himalaya: Role of long-range transport, *Atmospheric Environment*, 287, 119263,  
1116 <https://doi.org/10.1016/j.atmosenv.2022.119263>, 2022.
- 1117 Pervez, S., Bano, S., Watson, J. G., Chow, J. C., Matawle, J. L., Shrivastava, A., Tiwari, S., and Pervez,  
1118 Y. F.: Source profiles for PM<sup>10-2.5</sup> resuspended dust and vehicle exhaust emissions in Central India,  
1119 *Aerosol and Air Quality Research*, 18, 1660-1672, 10.4209/aaqr, 2018.
- 1120 Pio, C., Cerqueira, M., Harrison, R. M., Nunes, T., Mirante, F., Alves, C., Oliveira, C., Sanchez de la  
1121 Campa, A., Artíñano, B., and Matos, M.: OC/EC ratio observations in Europe: Re-thinking the  
1122 approach for apportionment between primary and secondary organic carbon, *Atmospheric*  
1123 *Environment*, 45, 6121-6132, 10.1016/j.atmosenv, 2011.
- 1124 Popovicheva, O. B., Engling, G., Diapouli, E., Saraga, D., Persiantseva, N. M., Timofeev, M. A., Kireeva,  
1125 E. D., Shonija, N. K., Chen, S.-H., Nguyen, D. L., Eleftheriadis, K., and Lee, C.-T.: Impact of smoke  
1126 intensity on size-resolved aerosol composition and microstructure during the biomass burning  
1127 season in Northwest Vietnam, *Aerosol and Air Quality Research*, 16, 2635-2654, 10.4209/aaqr,  
1128 2016.
- 1129 Qi, S., Zhao, S., Yu, Y., and Yang, L.: Composition, sources and potential source regions of aerosols  
1130 under contrasting environment conditions of Lanzhou, a valley city of western China: Observations  
1131 by means of topographic relief, *Atmospheric Pollution Research*, 15, 102154,  
1132 <https://doi.org/10.1016/j.apr, 2024>.
- 1133 Qiao, Q., Huang, B., Zhang, C., Piper, J. D. A., Pan, Y., and Sun, Y.: Assessment of heavy metal  
1134 contamination of dustfall in northern China from integrated chemical and magnetic investigation,  
1135 *Atmospheric Environment*, 74, 182-193, 10.1016/j.atmosenv, 2013.



- 1136 Ravindra, K., Kaur-Sidhu, M., Mor, S., and John, S.: Trend in household energy consumption pattern in  
1137 India: A case study on the influence of socio-cultural factors for the choice of clean fuel use, *Journal*  
1138 *of Cleaner Production*, 213, 1024-1034, <https://doi.org/10.1016/j.jclepro>, 2019.
- 1139 Reff, A., Eberly, S. I., and Bhawe, P. V.: Receptor modeling of ambient particulate matter data using  
1140 Positive Matrix Factorization: Review of existing methods, *Journal of the Air & Waste Management*  
1141 *Association*, 57, 146-154, [10.1080/10473289](https://doi.org/10.1080/10473289), 2007.
- 1142 Sandrini, S., Fuzzi, S., Piazzalunga, A., Prati, P., Bonasoni, P., Cavalli, F., Bove, M. C., Calvello, M.,  
1143 Cappelletti, D., Colombi, C., Contini, D., de Gennaro, G., Di Gilio, A., Fermo, P., Ferrero, L.,  
1144 Gianelle, V., Giugliano, M., Ielpo, P., Lonati, G., Marinoni, A., Massabò, D., Molteni, U., Moroni,  
1145 B., Pavese, G., Perrino, C., Perrone, M. G., Perrone, M. R., Putaud, J.-P., Sargolini, T., Vecchi, R.,  
1146 and Gilardoni, S.: Spatial and seasonal variability of carbonaceous aerosol across Italy, *Atmospheric*  
1147 *Environment*, 99, 587-598, <https://doi.org/10.1016/j.atmosenv>, 2014.
- 1148 Saud, T., Saxena, M., Singh, D. P., Saraswati, Dahiya, M., Sharma, S. K., Datta, A., Gadi, R., and Mandal,  
1149 T. K.: Spatial variation of chemical constituents from the burning of commonly used biomass fuels  
1150 in rural areas of the Indo-Gangetic Plain (IGP), India, *Atmospheric Environment*, 71, 158-169,  
1151 <https://doi.org/10.1016/j.atmosenv>, 2013.
- 1152 Schmidl, C., Marr, I. L., Caseiro, A., Kotianová, P., Berner, A., Bauer, H., Kasper-Giebl, A., and Puxbaum,  
1153 H.: Chemical characterisation of fine particle emissions from wood stove combustion of common  
1154 woods growing in mid-European Alpine regions, *Atmospheric Environment*, 42, 126-141,  
1155 <https://doi.org/10.1016/j.atmosenv>, 2008.
- 1156 Secrest, M. H., Schauer, J. J., Carter, E. M., and Baumgartner, J.: Particulate matter chemical component  
1157 concentrations and sources in settings of household solid fuel use, *Indoor Air*, 27, 1052-1066,  
1158 [10.1111/ina.12389](https://doi.org/10.1111/ina.12389), 2017.
- 1159 Seinfeld, J. H., Pandis, S. N., and Noone, K. J. J. P. T.: Atmospheric chemistry and physics: From air  
1160 pollution to climate change, 51, 88-90, 1998.
- 1161 Sheehan, P. E. and Bowman, F. M.: Estimated effects of temperature on secondary organic aerosol  
1162 concentrations, *Environmental Science & Technology*, 35, 2129-2135, [10.1021/es001547g](https://doi.org/10.1021/es001547g), 2001.
- 1163 Shen, G., Ru, M., Du, W., Zhu, X., Zhong, Q., Chen, Y., Shen, H., Yun, X., Meng, W., Liu, J., Cheng, H.,  
1164 Hu, J., Guan, D., and Tao, S.: Impacts of air pollutants from rural Chinese households under the  
1165 rapid residential energy transition, *Nature Communication*, 10, 3405, [10.1038/s41467-019-11453-](https://doi.org/10.1038/s41467-019-11453-)



- 1166 w, 2019.
- 1167 Shen, G.-F., Xiong, R., Cheng, H.-F and Tao, S.: Estimation of residential energy structure and primary  
1168 PM<sub>2.5</sub> emissions in rural Tibet (in Chinese), *Science Bulletin*, 66(15), 1900-1911, 2021.
- 1169 Shen, Z., Arimoto, R., Cao, J., Zhang, R., Li, X., Du, N., Okuda, T., Nakao, S., and Tanaka, S.: Seasonal  
1170 variations and evidence for the effectiveness of pollution controls on water-soluble inorganic species  
1171 in total suspended particulates and fine particulate matter from Xi'an, China, *Journal of the Air &  
1172 Waste Management Association*, 58, 1560-1570, 10.3155/1047-3289.58.12.1560, 2008.
- 1173 Shi, Z., Vu, T., Kotthaus, S., Harrison, R. M., Grimmond, S., Yue, S., Zhu, T., Lee, J., Han, Y., Demuzere,  
1174 M., Dunmore, R. E., Ren, L., Liu, D., Wang, Y., Wild, O., Allan, J., Acton, W. J., Barlow, J., Barratt,  
1175 B., Beddows, D., Bloss, W. J., Calzolari, G., Carruthers, D., Carslaw, D. C., Chan, Q., Chatzidiakou,  
1176 L., Chen, Y., Crilley, L., Coe, H., Dai, T., Doherty, R., Duan, F., Fu, P., Ge, B., Ge, M., Guan, D.,  
1177 Hamilton, J. F., He, K., Heal, M., Heard, D., Hewitt, C. N., Hollaway, M., Hu, M., Ji, D., Jiang, X.,  
1178 Jones, R., Kalberer, M., Kelly, F. J., Kramer, L., Langford, B., Lin, C., Lewis, A. C., Li, J., Li, W.,  
1179 Liu, H., Liu, J., Loh, M., Lu, K., Lucarelli, F., Mann, G., McFiggans, G., Miller, M. R., Mills, G.,  
1180 Monk, P., Nemitz, E., O'Connor, F., Ouyang, B., Palmer, P. I., Percival, C., Popoola, O., Reeves, C.,  
1181 Rickard, A. R., Shao, L., Shi, G., Spracklen, D., Stevenson, D., Sun, Y., Sun, Z., Tao, S., Tong, S.,  
1182 Wang, Q., Wang, W., Wang, X., Wang, X., Wang, Z., Wei, L., Whalley, L., Wu, X., Wu, Z., Xie, P.,  
1183 Yang, F., Zhang, Q., Zhang, Y., Zhang, Y., and Zheng, M.: Introduction to the special issue "In-depth  
1184 study of air pollution sources and processes within Beijing and its surrounding region (APHH-  
1185 Beijing)", *Atmospheric Chemistry and Physics*, 19, 7519-7546, 10.5194/acp-19-7519-2019, 2019.
- 1186 Simoneit, B. R. T.: Biomass burning — a review of organic tracers for smoke from incomplete  
1187 combustion, *Applied Geochemistry*, 17, 129-162, [https://doi.org/10.1016/S0883-2927\(01\)00061-0](https://doi.org/10.1016/S0883-2927(01)00061-0),  
1188 2002.
- 1189 Sow, M., Goossens, D., and Rajot, J. L.: Calibration of the MDCO dust collector and of four versions of  
1190 the inverted frisbee dust deposition sampler, *Geomorphology*, 82, 360-375,  
1191 10.1016/j.geomorph.2006.05.013, 2006.
- 1192 Strader, R., Lurmann, F., and Pandis, S. N.: Evaluation of secondary organic aerosol formation in winter,  
1193 *Atmospheric Environment*, 33, 4849-4863, [https://doi.org/10.1016/S1352-2310\(99\)00310-6](https://doi.org/10.1016/S1352-2310(99)00310-6), 1999.
- 1194 Sulong, N. A., Latif, M. T., Sahani, M., Khan, M. F., Fadzil, M. F., Tahir, N. M., Mohamad, N., Sakai,  
1195 N., Fujii, Y., Othman, M., and Tohno, S.: Distribution, sources and potential health risks of



- 1196 polycyclic aromatic hydrocarbons (PAHs) in PM<sub>2.5</sub> collected during different monsoon seasons and  
1197 haze episode in Kuala Lumpur, Chemosphere, 219, 1-14, 10.1016/j.chemosphere, 2019.
- 1198 Tang, Y., Han, G.-L and Xu, Z.-F.: Characteristics of black carbon content in atmospheric dust in Beijing  
1199 and its northern regions (in Chinese), Acta Scientiae Circumstantiae, 33(02), 332-338,  
1200 10.13671/j.hjkxxb.2013.02.033, 2013.
- 1201 Tao, J., Cheng, T., Zhang, R., Cao, J., Zhu, L., Wang, Q., Luo, L., and Zhang, L.: Chemical composition  
1202 of PM<sub>2.5</sub> at an urban site of Chengdu in southwestern China, Advances in Atmospheric Sciences, 30,  
1203 1070-1084, 10.1007/s00376-012-2168-7, 2013.
- 1204 Tao, S., Ru, M. Y., Du, W., Zhu, X., Zhong, Q. R., Li, B. G., Shen, G. F., Pan, X. L., Meng, W. J., Chen,  
1205 Y. L., Shen, H. Z., Lin, N., Su, S., Zhuo, S. J., Huang, T. B., Xu, Y., Yun, X., Liu, J. F., Wang, X. L.,  
1206 Liu, W. X., Cheng, H. F., and Zhu, D. Q.: Quantifying the rural residential energy transition in China  
1207 from 1992 to 2012 through a representative national survey, Nature Energy, 3, 567-573,  
1208 10.1038/s41560-018-0158-4, 2018.
- 1209 Tian, M., Gao, J., Zhang, L., Zhang, H., Feng, C., and Jia, X.: Effects of dust emissions from wind erosion  
1210 of soil on ambient air quality, Atmospheric Pollution Research, 12, 10.1016/j.apr.2021.101108, 2021.
- 1211 Turpin, B. J. and Huntzicker, J. J.: Secondary formation of organic aerosol in the Los Angeles basin: A  
1212 descriptive analysis of organic and elemental carbon concentrations, Atmospheric Environment.  
1213 Part A. General Topics, 25, 207-215, [https://doi.org/10.1016/0960-1686\(91\)90291-E](https://doi.org/10.1016/0960-1686(91)90291-E), 1991.
- 1214 Turpin, B. J. and Huntzicker, J. J.: Identification of secondary organic aerosol episodes and quantitation  
1215 of primary and secondary organic aerosol concentrations during SCAQS, Atmospheric Environment,  
1216 29, 3527-3544, [https://doi.org/10.1016/1352-2310\(94\)00276-Q](https://doi.org/10.1016/1352-2310(94)00276-Q), 1995.
- 1217 VanCuren, R. and Gustin, M. S.: Identification of sources contributing to PM<sub>2.5</sub> and ozone at elevated  
1218 sites in the western U.S. by receptor analysis: Lassen Volcanic National Park, California, and Great  
1219 Basin National Park, Nevada, Science of The Total Environment, 530-531, 505-518,  
1220 <https://doi.org/10.1016/j.scitotenv>, 2015.
- 1221 Wang, F., Michalski, G., Seo, J.-h., and Ge, W.: Geochemical, isotopic, and mineralogical constraints on  
1222 atmospheric deposition in the hyper-arid Atacama Desert, Chile, Geochimica et Cosmochimica Acta,  
1223 135, 29-48, <https://doi.org/10.1016/j.gca>, 2014.
- 1224 Wang, J., Yu, A., Yang, L., and Fang, C.: Research on organic carbon and elemental carbon distribution  
1225 characteristics and their influence on fine particulate matter (PM<sub>2.5</sub>) in Changchun City,



- 1226 10.3390/environments6020021, 2019.
- 1227 Wang, Z.-Y., Xue, D., Jia, H.-Y., Liu, J., Mao, T.-Y., Song, S.-J. and Li, H.-P.: Characteristics of  
1228 carbonaceous components in atmospheric fine particulate matter in Binhai New Area, Tianjin (in  
1229 Chinese), *Environmental Chemistry*, 40: 1871-1876, 2021.
- 1230 Wei, N., Ma, C., Liu, J., Wang, G., Liu, W., Zhuoga, D., Xiao, D., and Yao, J.: Size-segregated  
1231 characteristics of carbonaceous aerosols during the monsoon and non-monsoon seasons in Lhasa in  
1232 the Tibetan Plateau, 10.3390/atmos10030157, 2019.
- 1233 Wei, T., Dong, Z., Kang, S., Qin, X., and Guo, Z.: Geochemical evidence for sources of surface dust  
1234 deposited on the Laohugou glacier, Qilian Mountains, *Applied Geochemistry*, 79, 1-8,  
1235 <https://doi.org/10.1016/j.apgeochem>, 2017.
- 1236 Wu, C. and Yu, J. Z.: Determination of primary combustion source organic carbon-to-elemental carbon  
1237 (OC/EC) ratio using ambient OC and EC measurements: secondary OC-EC correlation  
1238 minimization method, *Atmospheric Chemistry and Physics*, 16, 5453-5465, 10.5194/acp-16-5453-  
1239 2016, 2016.
- 1240 Wu, C., Wu, D., and Yu, J. Z.: Quantifying black carbon light absorption enhancement with a novel  
1241 statistical approach, *Atmospheric Chemistry and Physics*, 18, 289-309, 10.5194/acp-18-289-2018,  
1242 2018a.
- 1243 Wu, G., Wan, X., Gao, S., Fu, P., Yin, Y., Li, G., Zhang, G., Kang, S., Ram, K., and Cong, Z.: Humic-  
1244 Like Substances (HULIS) in aerosols of Central Tibetan Plateau (Nam Co, 4730 m asl): Abundance,  
1245 light absorption properties, and sources, *Environmental Science & Technology*, 52, 7203-7211,  
1246 10.1021/acs.est.8b01251, 2018b.
- 1247 Xia, X., Zong, X., Cong, Z., Chen, H., Kang, S., and Wang, P.: Baseline continental aerosol over the  
1248 central Tibetan plateau and a case study of aerosol transport from South Asia, *Atmospheric*  
1249 *Environment*, 45, 7370-7378, <https://doi.org/10.1016/j.atmosenv>.2011.07.067, 2011.
- 1250 Xiang, Y., Li, X., Zhang, T., Cheng, Q., Yan, C., Liu, X., Liu, Y., Wang, Y., Kang, S., Ding, X., and Zheng,  
1251 M.: Characteristics and sources of organic aerosol in PM<sub>2.5</sub> at Yangbajing in Tibetan Plateau,  
1252 *Atmospheric Environment*, 333, 120662, <https://doi.org/10.1016/j.atmosenv>, 2024.
- 1253 Xiao, Q., Saikawa, E., Yokelson, R. J., Chen, P., Li, C., and Kang, S.: Indoor air pollution from burning  
1254 yak dung as a household fuel in Tibet, *Atmospheric Environment*, 102, 406-412, 10.1016/j.atmosenv,  
1255 2015.





- 1256 Xie, F., Guo, L., Wang, Z., Tian, Y., Yue, C., Zhou, X., Wang, W., Xin, J., and Lu, C.: Geochemical  
1257 characteristics and socioeconomic associations of carbonaceous aerosols in coal-fueled cities with  
1258 significant seasonal pollution pattern, *Environ Int*, 179, 108179, 10.1016/j.envint.2023.108179,  
1259 2023.
- 1260 Xu, J., Wang, Q., Deng, C., McNeill, V. F., Fankhauser, A., Wang, F., Zheng, X., Shen, J., Huang, K., and  
1261 Zhuang, G.: Insights into the characteristics and sources of primary and secondary organic carbon:  
1262 High time resolution observation in urban Shanghai, *Environmental Pollution*, 233, 1177-1187,  
1263 [https://doi.org/10.1016/j.envpol](https://doi.org/10.1016/j.envpol.2018a), 2018a.
- 1264 Xu, J. Z., Zhang, Q., Wang, Z. B., Yu, G. M., Ge, X. L., and Qin, X.: Chemical composition and size  
1265 distribution of summertime PM<sub>2.5</sub> at a high altitude remote location in the northeast of the Qinghai–  
1266 Xizang (Tibet) Plateau: insights into aerosol sources and processing in free troposphere,  
1267 *Atmospheric Chemistry and Physics*, 15, 5069-5081, 10.5194/acp-15-5069-2015, 2015.
- 1268 Xu, L., Chen, X., Chen, J., Zhang, F., He, C., Zhao, J., and Yin, L.: Seasonal variations and chemical  
1269 compositions of PM<sub>2.5</sub> aerosol in the urban area of Fuzhou, China, *Atmospheric Research*, 104-  
1270 105, 264-272, [https://doi.org/10.1016/j.atmosres](https://doi.org/10.1016/j.atmosres.2012), 2012.
- 1271 Xu, R., Tie, X., Li, G., Zhao, S., Cao, J., Feng, T., and Long, X.: Effect of biomass burning on black  
1272 carbon (BC) in South Asia and Tibetan Plateau: The analysis of WRF-Chem modeling, *Science of  
1273 The Total Environment*, 645, 901-912, <https://doi.org/10.1016/j.scitotenv.2018.07.165>, 2018b.
- 1274 Xue, W., Wang, L., Yang, Z., Xiong, Z., Li, X., Xu, Q., and Cai, Z.: Can clean heating effectively alleviate  
1275 air pollution: An empirical study based on the plan for cleaner winter heating in northern China,  
1276 *Applied Energy*, 351, 121923, [https://doi.org/10.1016/j.apenergy](https://doi.org/10.1016/j.apenergy.2023), 2023.
- 1277 Yang, F., He, K., Ye, B., Chen, X., Cha, L., Cadle, S. H., Chan, T., and Mulawa, P. A.: One-year record  
1278 of organic and elemental carbon in fine particles in downtown Beijing and Shanghai, *Atmospheric  
1279 Chemistry and Physics*, 5, 1449-1457, 10.5194/acp-5-1449-2005, 2005.
- 1280 Yang, Q.-L., Wang, J.-X and Zhao, Z.-X.: Temporal and spatial distribution characteristics and source  
1281 analysis of heavy metals in atmospheric dust in typical industrial cities in Northeast China during  
1282 winter and spring (in Chinese), *Acta Scientiae Circumstantiae*, 1-9, 10.13671/j.hjkxxb.2024.0254,  
1283 2024.
- 1284 Yang, X.-Y.: Analysis of the current status of atmospheric environment in the Northwest China region  
1285 (Gansu-Qinghai-New) (in Chinese), Master's thesis, Lanzhou University, 2014.



- 1286 Yao, L., Yang, L., Yuan, Q., Yan, C., Dong, C., Meng, C., Sui, X., Yang, F., Lu, Y., and Wang, W.: Sources  
1287 apportionment of PM<sub>2.5</sub> in a background site in the North China Plain, Science of the Total  
1288 Environment, 541, 590-598, 10.1016/j.scitotenv, 2016a.
- 1289 Yao, L., Yang, L., Yuan, Q., Yan, C., Dong, C., Meng, C., Sui, X., Yang, F., Lu, Y., and Wang, W.: Sources  
1290 apportionment of PM<sub>2.5</sub> in a background site in the North China Plain, Science of The Total  
1291 Environment, 541, 590-598, <https://doi.org/10.1016/j.scitotenv>, 2016b.
- 1292 Ye, W., Saikawa, E., Avramov, A., Cho, S. H., and Chartier, R.: Household air pollution and personal  
1293 exposure from burning firewood and yak dung in summer in the eastern Tibetan Plateau,  
1294 Environmental Pollution, 263, 114531, 10.1016/j.envpol, 2020.
- 1295 Yu, H., Yang, W., Wang, X., Yin, B., Zhang, X., Wang, J., Gu, C., Ming, J., Geng, C., and Bai, Z.: A  
1296 seriously sand storm mixed air-polluted area in the margin of Tarim Basin: Temporal-spatial  
1297 distribution and potential sources, Science of The Total Environment, 676, 436-446,  
1298 <https://doi.org/10.1016/j.scitotenv>, 2019.
- 1299 Yu, L.-P., Li, D., Meng, L., Du, C.-Y. and Zhao, P.: Observation and data processing methods for  
1300 atmospheric dust deposition (in Chinese), Anhui Agricultural Sciences, 44: 185-186,  
1301 10.13989/j.cnki.0517-6611.2016.31.064, 2016.
- 1302 Zhan, C.-L., Zhan, J.-W., Ke, Z.-D., Liu, S., Zhang, J.-Q and Liu, H.-X.: Pollution characteristics and  
1303 source analysis of black carbon in different types of dust in Xiaogan, Hubei (in Chinese),  
1304 Environmental Pollution and Control 44(01), 14-19 + 26, 10.15985/j.cnki.1001-3865, 2022.
- 1305 Zhan, C.-L., Zhang, J.-Q., Zheng, J.-G., Yao, R.-Z., Xiao, W.-S and Cao, J.-J.: Pollution characteristics  
1306 and source analysis of black carbon in atmospheric dust along National Highway 316 (in Chinese),  
1307 Environmental Science and Technology, 39(04), 154-160, 2016.
- 1308 Zhang, F.: Study on the dry deposition of organic carbon and elemental carbon in the atmosphere of  
1309 Nanchang (in Chinese), Master's Thesis, 2014.
- 1310 Zhang, F., Wang, Z.-w., Cheng, H.-r., Lv, X.-p., Gong, W., Wang, X.-m., and Zhang, G.: Seasonal  
1311 variations and chemical characteristics of PM<sub>2.5</sub> in Wuhan, central China, Science of The Total  
1312 Environment, 518-519, 97-105, <https://doi.org/10.1016/j.scitotenv>, 2015a.
- 1313 Zhang, F., Wang, Z. W., Cheng, H. R., Lv, X. P., Gong, W., Wang, X. M., and Zhang, G.: Seasonal  
1314 variations and chemical characteristics of PM<sub>2.5</sub> in Wuhan, central China, Science of the Total  
1315 Environment, 518-519, 97-105, 10.1016/j.scitotenv, 2015b.



- 1316 Zhang, J., Smith, K. R., Ma, Y., Ye, S., Jiang, F., Qi, W., Liu, P., Khalil, M. A. K., Rasmussen, R. A., and  
1317 Thorneloe, S. A.: Greenhouse gases and other airborne pollutants from household stoves in China:  
1318 a database for emission factors, *Atmospheric Environment*, 34, 4537-4549,  
1319 [https://doi.org/10.1016/S1352-2310\(99\)00450-1](https://doi.org/10.1016/S1352-2310(99)00450-1), 2000.
- 1320 Zhang, K., Shang, X., Herrmann, H., Meng, F., Mo, Z., Chen, J., and Lv, W.: Approaches for identifying  
1321 PM<sub>2.5</sub> source types and source areas at a remote background site of South China in spring, *Science*  
1322 *of The Total Environment*, 691, 1320-1327, <https://doi.org/10.1016/j.scitotenv>, 2019.
- 1323 Zhang, N., Cao, J., Liu, S., Zhao, Z., Xu, H., and Xiao, S.: Chemical composition and sources of PM<sub>2.5</sub>  
1324 and TSP collected at Qinghai Lake during summertime, *Atmospheric Research*, 138, 213-222,  
1325 <https://doi.org/10.1016/j.atmosres>, 2014.
- 1326 Zhang, N.-N., He, Y.-Q., Wang, C.-F., Pang, H.-X., He, X.-Z.: The impact of tourism industry  
1327 development on the chemical characteristics of atmospheric precipitation: a case study of Lijiang,  
1328 Yunnan (in Chinese), *Environmental Science*, 32(02), 330-337, 10.13227/j.hjkx, 2011.
- 1329 Zhang, P.-X.: Salt lakes in the Qaidam Basin (in Chinese), Beijing: Science Press, 1987.
- 1330 Zhang, R.-J., Cao, J.-j., Lee, S.-c., Shen, Z.-x., and Ho, K.-F.: Carbonaceous aerosols in PM<sub>10</sub> and  
1331 pollution gases in winter in Beijing, *Journal of Environmental Sciences*, 19, 564-571,  
1332 [https://doi.org/10.1016/S1001-0742\(07\)60094-1](https://doi.org/10.1016/S1001-0742(07)60094-1), 2007.
- 1333 Zhang, R., Wang, H., Qian, Y., Rasch, P. J., Easter, R. C., Ma, P. L., Singh, B., Huang, J., and Fu, Q.:  
1334 Quantifying sources, transport, deposition, and radiative forcing of black carbon over the Himalayas  
1335 and Tibetan Plateau, *Atmospheric Chemistry and Physics*, 15, 6205-6223, 10.5194/acp-15-6205-  
1336 2015, 2015c.
- 1337 Zhang, X. Y., Wang, Y. Q., Zhang, X. C., Guo, W., and Gong, S. L.: Carbonaceous aerosol composition  
1338 over various regions of China during 2006, *Journal of Geophysical Research: Atmospheres*, 113,  
1339 10.1029/2007jd009525, 2008.
- 1340 Zhang, X. Y., Wang, Y. Q., Wang, D., Gong, S. L., Arimoto, R., Mao, L. J., and Li, J.: Characterization  
1341 and sources of regional-scale transported carbonaceous and dust aerosols from different pathways  
1342 in coastal and sandy land areas of China, *Journal of Geophysical Research: Atmospheres*, 110,  
1343 10.1029/2004jd005457, 2005.
- 1344 Zhang, Z., Zhou, Y., Zhao, N., Li, H., Tohniyaz, B., Mperejekumana, P., Hong, Q., Wu, R., Li, G., Sultan,  
1345 M., Zayan, A. M. I., Cao, J., Ahmad, R., and Dong, R.: Clean heating during winter season in



- 1346 Northern China: A review, *Renewable and Sustainable Energy Reviews*, 149, 111339,  
1347 [https://doi.org/10.1016/j.rser](https://doi.org/10.1016/j.rser.2021), 2021.
- 1348 Zhang, Z.-C., Xie, Y.-Q., Zhang, Z.-J., Gao, G.-S., Xu, B., Tian, X., Xu, H., Wie, Y.-T., Shi, G.-L. and  
1349 Feng, Y.-C.: Source analysis and seasonal variation characteristics of atmospheric dust deposition  
1350 in Taiyuan City based on two receptor models (in Chinese), *China Environmental Science*, 42, 2577-  
1351 2586, 10.3969/j.issn.1000-6923, 2022.
- 1352 Zhao, S., Qi, S., Yu, Y., Kang, S., Dong, L., Chen, J., and Yin, D.: Measurement report: Contrasting  
1353 elevation-dependent light absorption by black and brown carbon: lessons from in situ measurements  
1354 from the highly polluted Sichuan Basin to the pristine Tibetan Plateau, *Atmospheric Chemistry and*  
1355 *Physics*, 22, 14693-14708, 10.5194/acp-22-14693-2022, 2022.
- 1356 Zhao, Z., Wang, Q., Li, L., Han, Y., Ye, Z., Pongpiachan, S., Zhang, Y., Liu, S., Tian, R., and Cao, J.:  
1357 Characteristics of PM<sub>2.5</sub> at a high-altitude remote site in the southeastern margin of the Tibetan  
1358 Plateau in premonsoon season, 10.3390/atmos10110645, 2019.
- 1359 Zheng, J., Hu, M., Du, Z., Shang, D., Gong, Z., Qin, Y., Fang, J., Gu, F., Li, M., Peng, J., Li, J., Zhang,  
1360 Y., Huang, X., He, L., Wu, Y., and Guo, S.: Influence of biomass burning from South Asia at a high-  
1361 altitude mountain receptor site in China, *Atmospheric Chemistry and Physics*, 17, 6853-6864,  
1362 10.5194/acp-17-6853-2017, 2017.
- 1363 Zheng, K., Li, Y., Li, Z., and Huang, J.: Provenance tracing of dust using rare earth elements in recent  
1364 snow deposited during the pre-monsoon season from mountain glaciers in the central to northern  
1365 Tibetan Plateau, *Environmental Science and Pollution Research*, 28, 45765-45779, 10.1007/s11356-  
1366 021-13561-x, 2021.
- 1367 Zheng, M.-P.: Geological report on salt lake resources and ecological environment in China (in Chinese),  
1368 *Acta Geologica Sinica*, 84: 1613-1622. DOI: 10.19762/j.cnki.dizhixuebao, 2017.
- 1369 Zhou, Y., Gao, X., and Lei, J.: Characteristics of dust weather in the Tarim Basin from 1989 to 2021 and  
1370 its impact on the atmospheric environment, 10.3390/rs15071804, 2023.
- 1371 Zhou, Y., Yang, J., Kang, S., Hu, Y., Chen, X., Xu, M., and Ma, M.: Black carbon aerosols impact  
1372 snowfall over the Tibetan Plateau, *Geoscience Frontiers*, 16, 101978, <https://doi.org/10.1016/j.gsf>,  
1373 2025.
- 1374 Zhu, C.-S., Chen, C.-C., Cao, J.-J., Tsai, C.-J., Chou, C. C. K., Liu, S.-C., and Roam, G.-D.:  
1375 Characterization of carbon fractions for atmospheric fine particles and nanoparticles in a highway



- 1376 tunnel, Atmospheric Environment, 44, 2668-2673, 10.1016/j.atmosenv, 2010.
- 1377 Zhu, H., Li, W., Kong, X., and Zhang, X.: Overlooked contribution of salt lake emissions: A case study
- 1378 of dust deposition from the Qinghai-Xizang Plateau, Journal of Geophysical Research: Atmospheres,
- 1379 130, e2024JD042693, <https://doi.org/10.1029/2024JD042693>, 2025.
- 1380 Zhu, H.-X.: The dust deposition data of the Qaidam Basin [Data set]. Zenodo.
- 1381 <https://doi.org/10.5281/zenodo.14382853>, 2024.